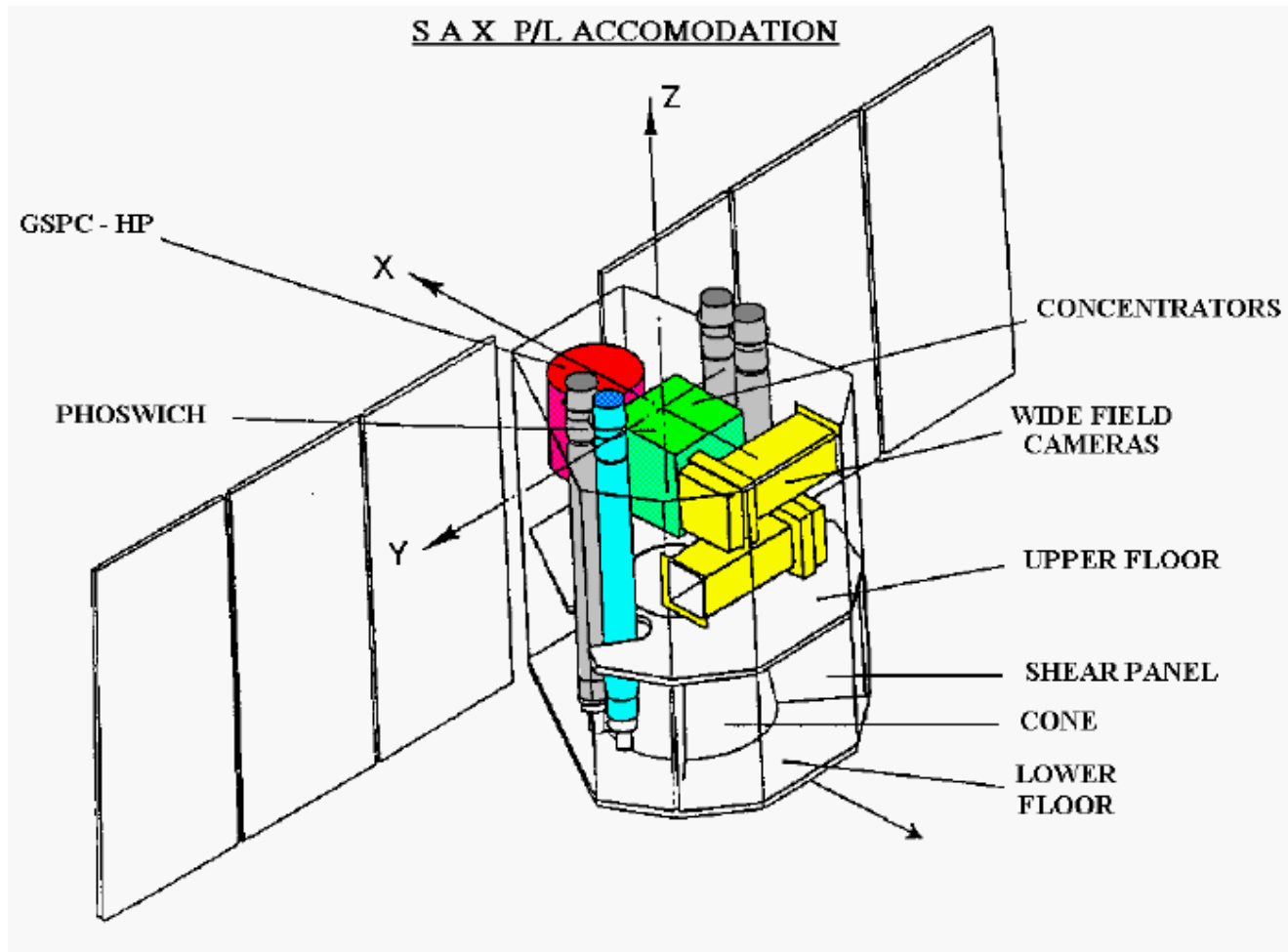


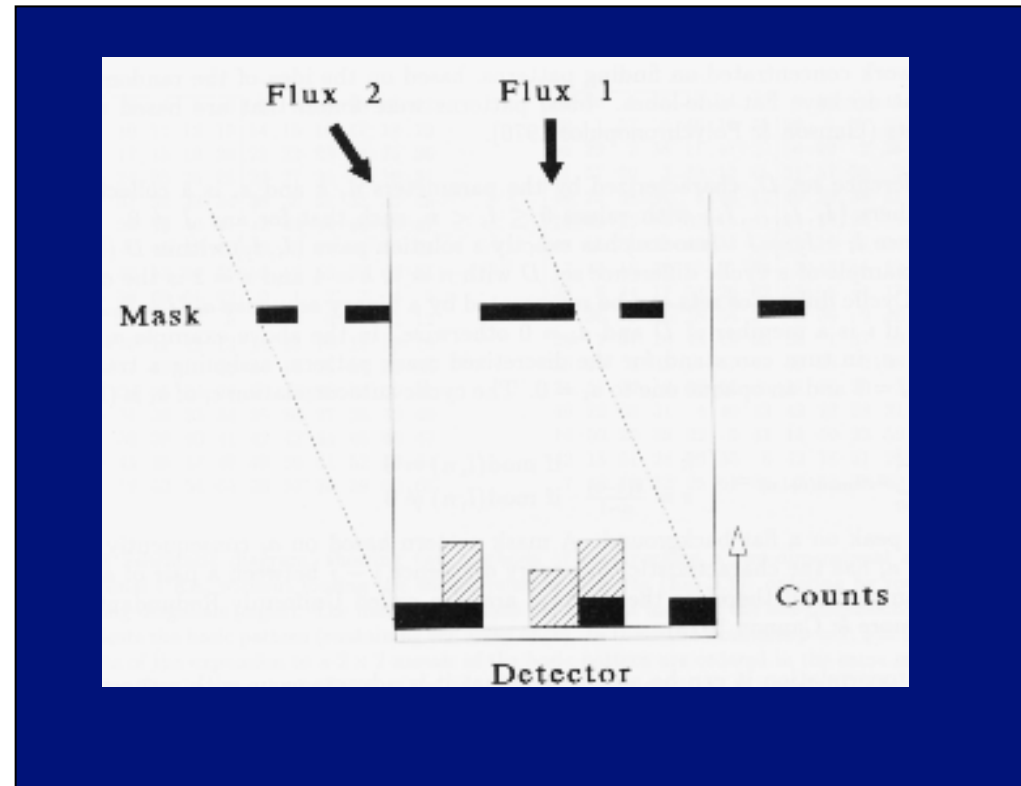
Astrofisica Nucleare e Subnucleare
Gamma ray Bursts – III

BeppoSAX (1995 - 2002)



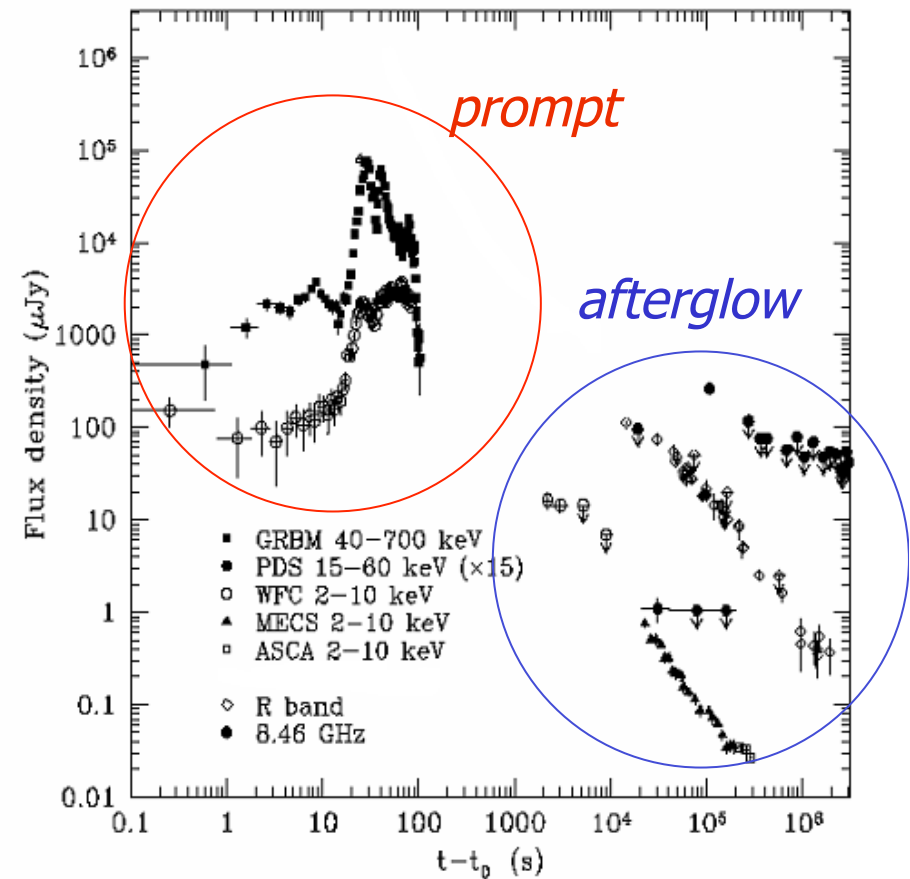
Coded Mask Imaging

The principle of the camera is straightforward: photons from a certain direction in the sky project the mask on the detector; this projection has the same coding as the mask pattern, but is shifted relative to the central position over a distance uniquely correspondent to the direction of the photons. The detector accumulates the sum of a number of shifted mask patterns. Each shift encodes the position and its strength encodes the intensity of the sky at that position.



http://asd.gsfc.nasa.gov/archive/cai/coded_intr.html

- in 1997, thanks to BeppoSAX observations, discovery of fading X-ray, optical, radio emission following the GRB
- photons received during the classical GRB phenomenon are then called “**prompt emission**” and the subsequent fading emission is called “**afterglow emission**”



Adapted from Maiorano et al.,
A&A, 2005

The compactness problem

$$R_i < c\delta t \quad \gamma\gamma \rightarrow e^+e^-$$

$$\tau_{\gamma\gamma} = \frac{f_p \sigma_T F D_L^2}{R_i^2 m_e c^2} \approx 10^{17} f_p \left(\frac{F}{10^{-6} \text{ erg/cm}^2} \right) \left(\frac{D_L}{3 \text{ Gpc}} \right)^2 \left(\frac{\delta t}{1 \text{ ms}} \right)$$

$$\tau_{\gamma\gamma} \gg 1$$

Very High Optical Depth to pair production

$$\Gamma = \frac{1}{\sqrt{1 - \beta^2}}$$

Size

Pair fraction

$$R_i < \Gamma^2 c\delta t \quad f_p \rightarrow f_p \Gamma^{-2\alpha}$$

$$\tau_{\gamma\gamma} = \frac{f_p \sigma_T F D_L^2}{R_i^2 m_e c^2} \approx \frac{10^{17}}{\Gamma^{4+2\alpha}} f_p \left(\frac{F}{10^{-6} \text{ erg/cm}^2} \right) \left(\frac{D_L}{3 \text{ Gpc}} \right)^2 \left(\frac{\delta t}{1 \text{ ms}} \right)$$

$$\Gamma \approx 10^2 \div 10^3$$

Piran (1999)

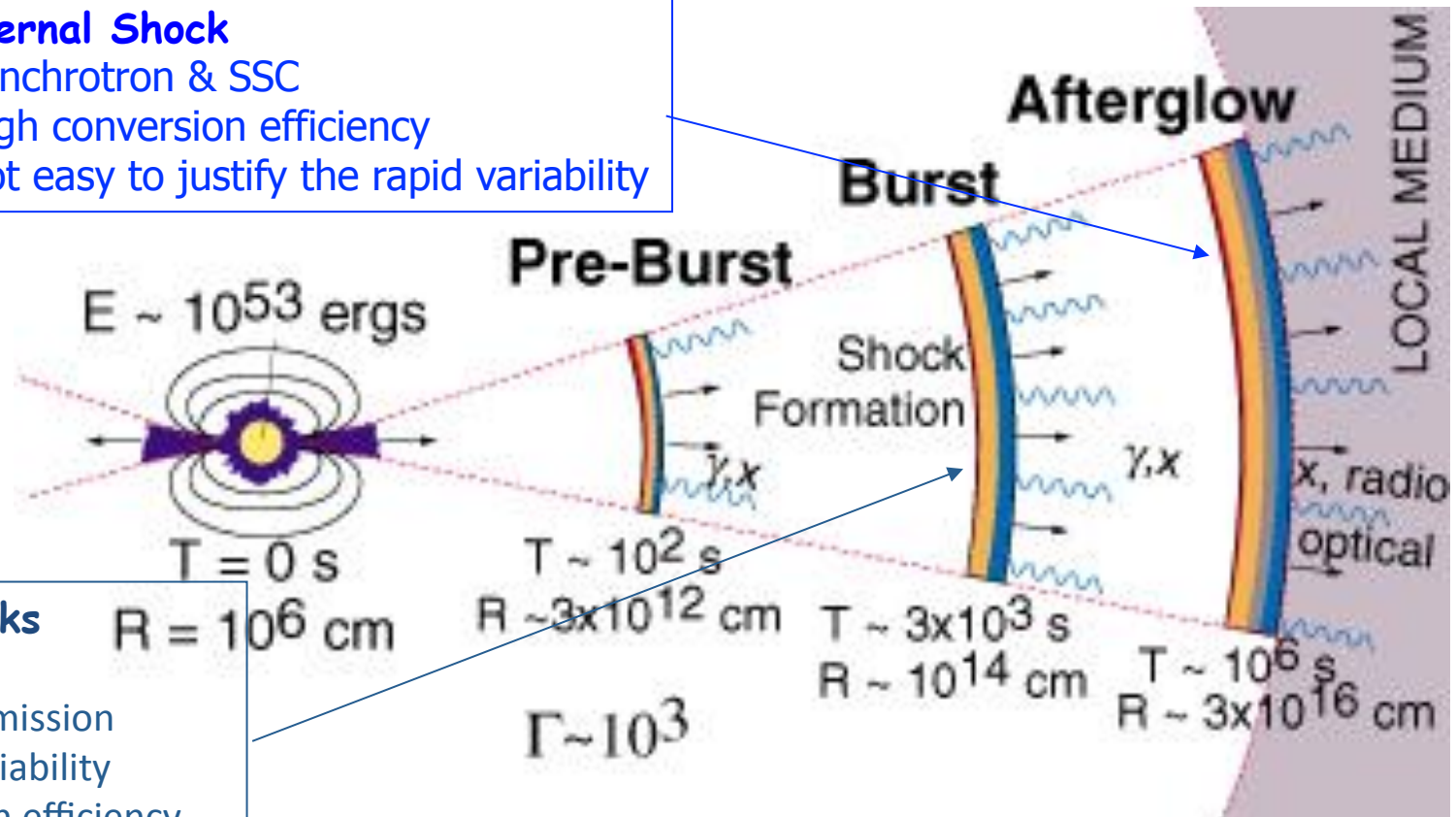
Relativistic motion of the emitting region ⁵

The Fireball model

- Relativistic motion of the emitting region
- Shock mechanism converts the kinetic energy of the shells into radiation.
- Baryon Loading problem

External Shock

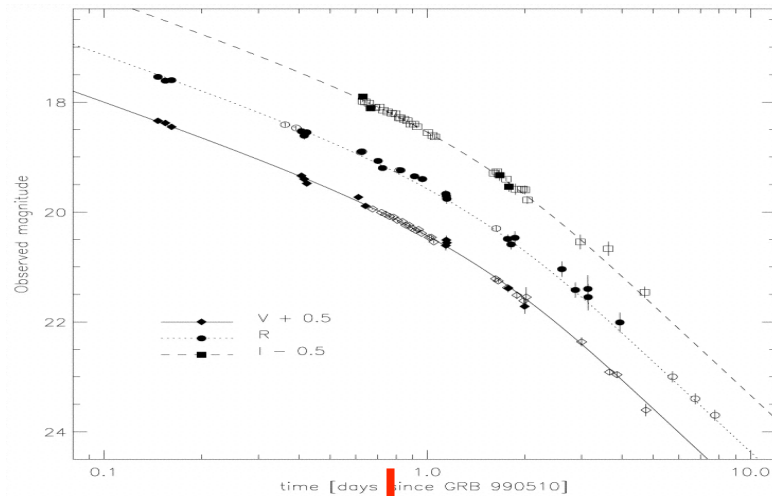
- Synchrotron & SSC
- High conversion efficiency
- Not easy to justify the rapid variability



Internal Shocks

- Source activity
- Synchrotron Emission
- Rapid time Variability
- Low conversion efficiency

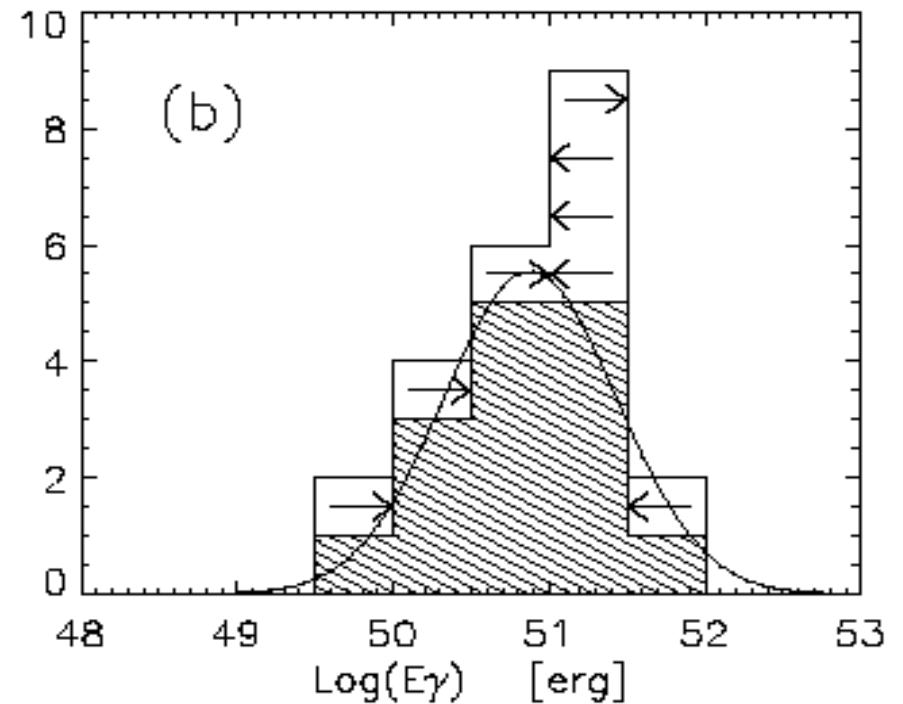
Jet breaks



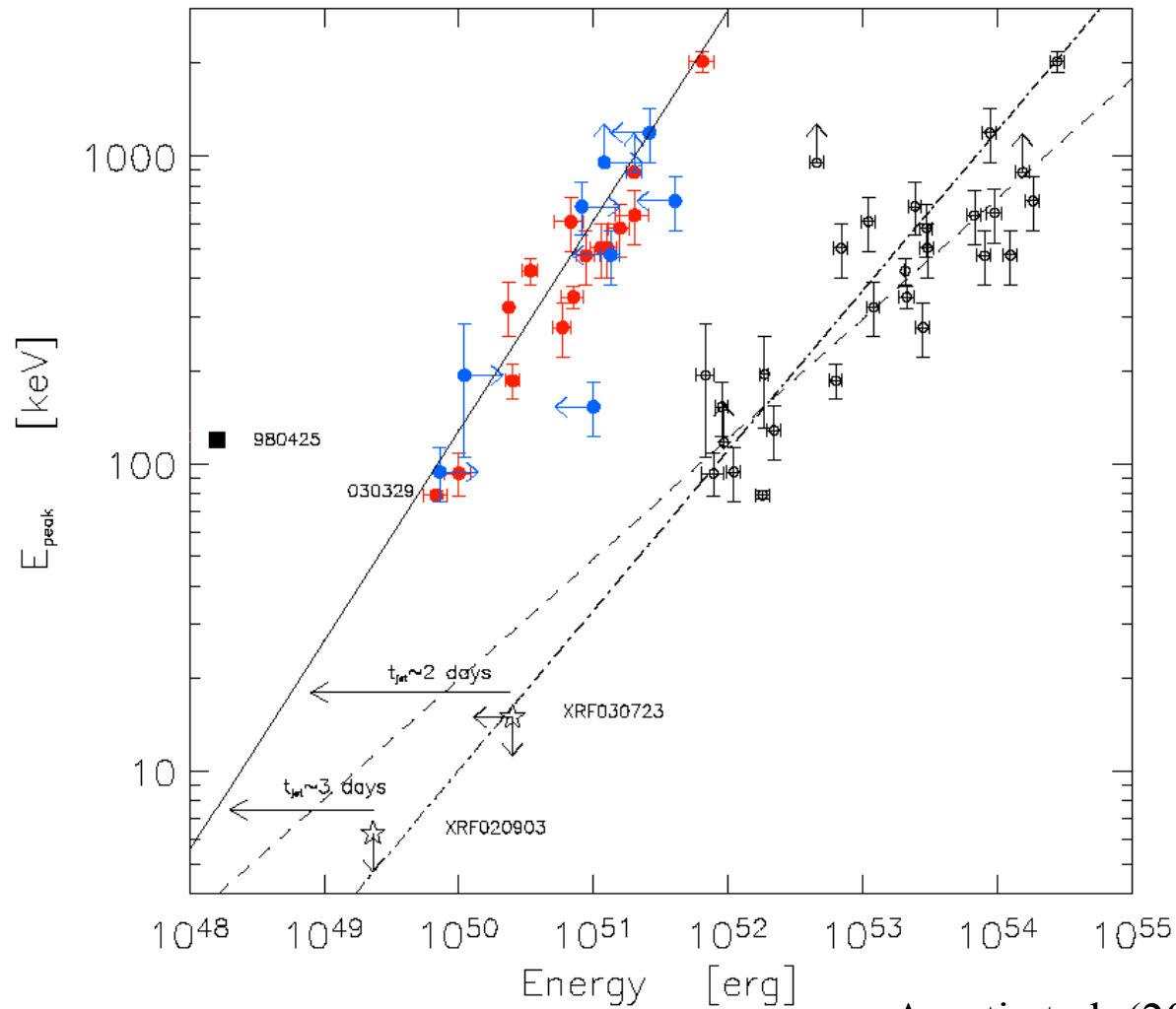
➤ breaks in the afterglow decay light curves -> collimation ?

$$\theta = 0.09 \left(\frac{t_{jet,d}}{1+z} \right)^{3/8} \left(\frac{n\eta_\gamma}{E_{\gamma,iso,52}} \right)^{1/8}$$

$$E_\gamma = (1 - \cos \theta) E_{\gamma,iso}$$



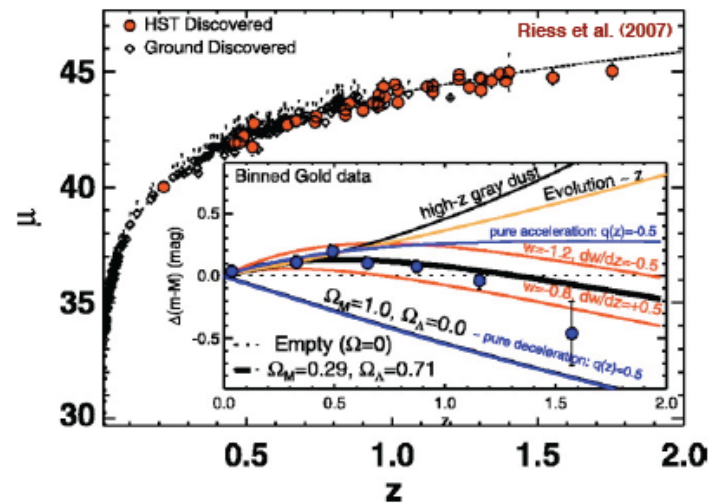
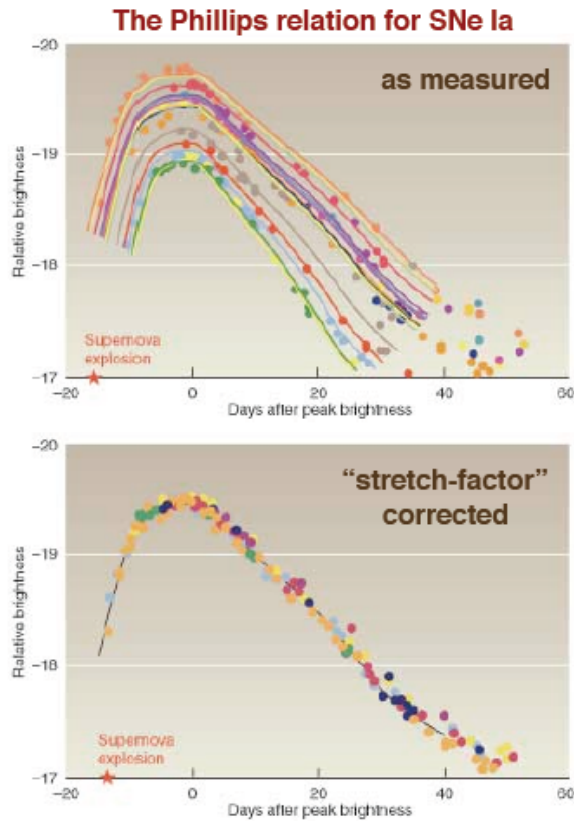
GRB for Cosmology



Amati et al. (2002)
Ghirlanda et al. (2004)

SN Ia Cosmology

SNe Ia as a “standard candle”



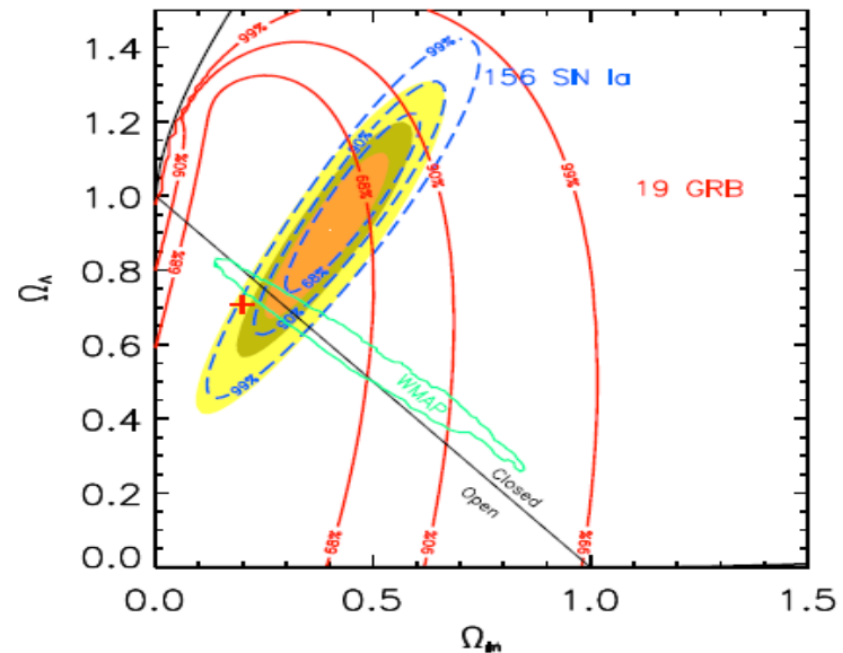
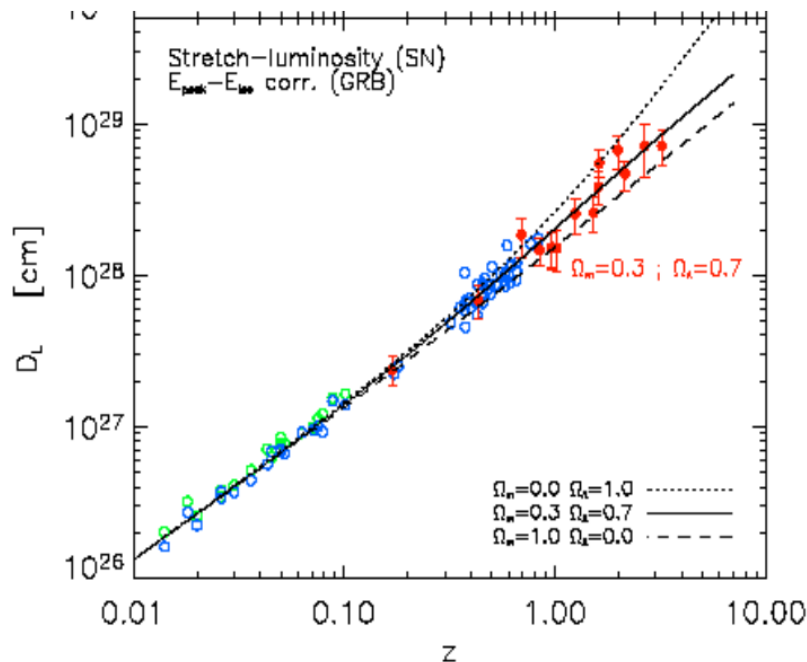
Can we apply GRBs as a standardized candle?

□ **Method** (e.g., Ghirlanda et al, Firmani et al., Dai et al., Zhang et al.):

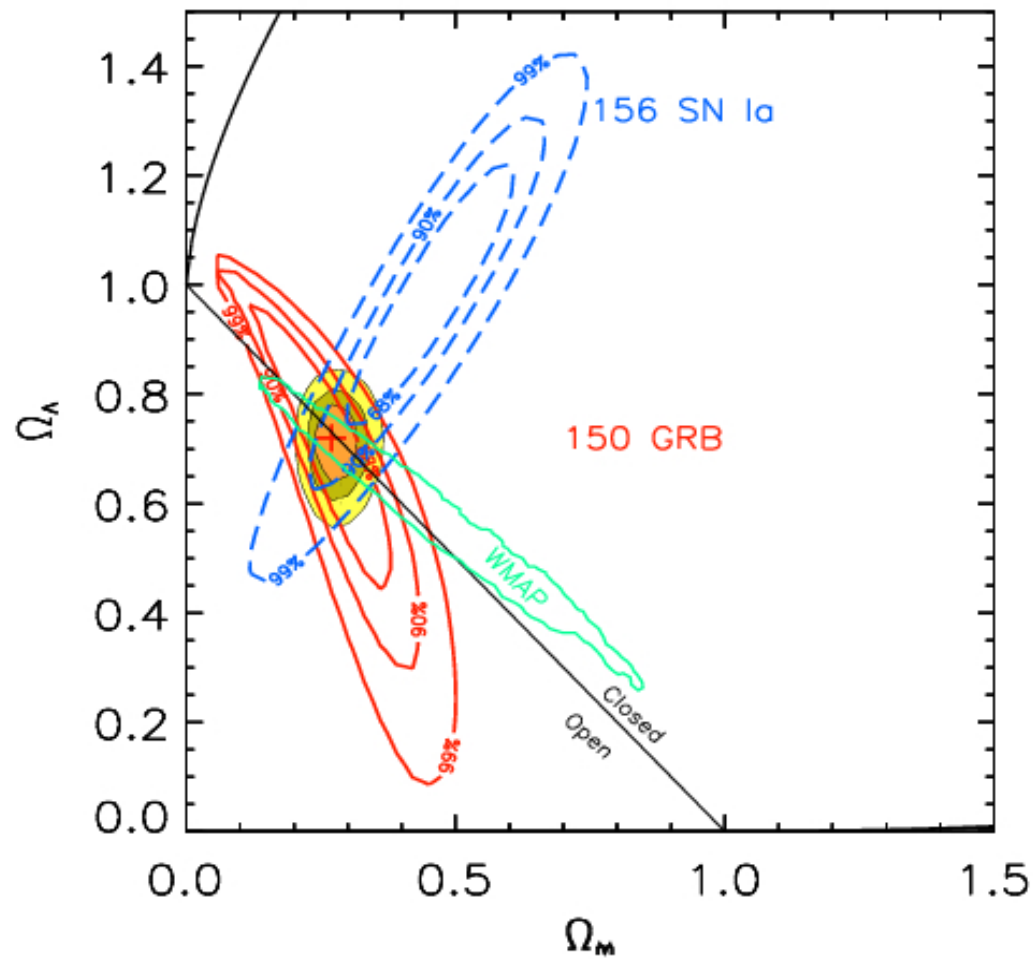
$$E_{p,i} = E_{p,obs} \times (1 + z), \quad t_{b,i} = t_b / (1 + z)$$

$$E_{\gamma,iso} = \frac{4\pi D_L^2}{(1+z)} \int_{1/(1+z)}^{10^4/(1+z)} E N(E) dE \quad \text{erg} \quad \rightarrow \quad D_L = D_L(z, H_0, \Omega_M, \Omega_\Lambda, \dots)$$

➤ fit the correlation and construct an Hubble diagram for each set of cosmological parameters -> derive c.l. contours based on chi-square



□ results obtainable with 150 GRBs with estimates of z , $E_{p,i}$ and t_b



Ghirlanda et al. 2006 A&A

Ghirlanda et al. 2006 JOP Review, GRB Special Issue

Luminosity distance

Distance measures in cosmology

DAVID W. HOGG

Institute for Advanced Study, 1 Einstein Drive, Princeton NJ 08540

`hogg@ias.edu`

2000 December

arXiv:astro-ph/9905116v4 16 Dec 2000

1 Introduction

In cosmology (or to be more specific, *cosmography*, the measurement of the Universe) there are many ways to specify the distance between two points, because in the expanding Universe, the distances between comoving objects are constantly changing, and Earth-bound observers look back in time as they look out in distance. The unifying aspect is that all distance measures somehow measure the separation between events on radial null trajectories, ie, trajectories of photons which terminate at the observer.

In this note, formulae for many different cosmological distance measures are provided. I treat the concept of “distance measure” very liberally, so, for instance, the lookback time and comoving volume are both considered distance measures. The bibliography of source material can be consulted for many of the derivations; this is merely a “cheat sheet.” Minimal *C* routines (KR) which compute all of these distance measures are available from the author upon request. Comments and corrections are highly appreciated, as are acknowledgments or citation in research that makes use of this summary or the associated code.

2 Cosmographic parameters

The *Hubble constant* H_0 is the constant of proportionality between recession speed v and distance d in the expanding Universe;

$$v = H_0 d \tag{1}$$

The subscripted “0” refers to the present epoch because in general H changes with time.

The Luminosity Distance

$$\Omega_M + \Omega_\Lambda + \Omega_k = 1 \quad z \equiv \frac{\nu_e}{\nu_o} - 1 = \frac{\lambda_o}{\lambda_e} - 1$$

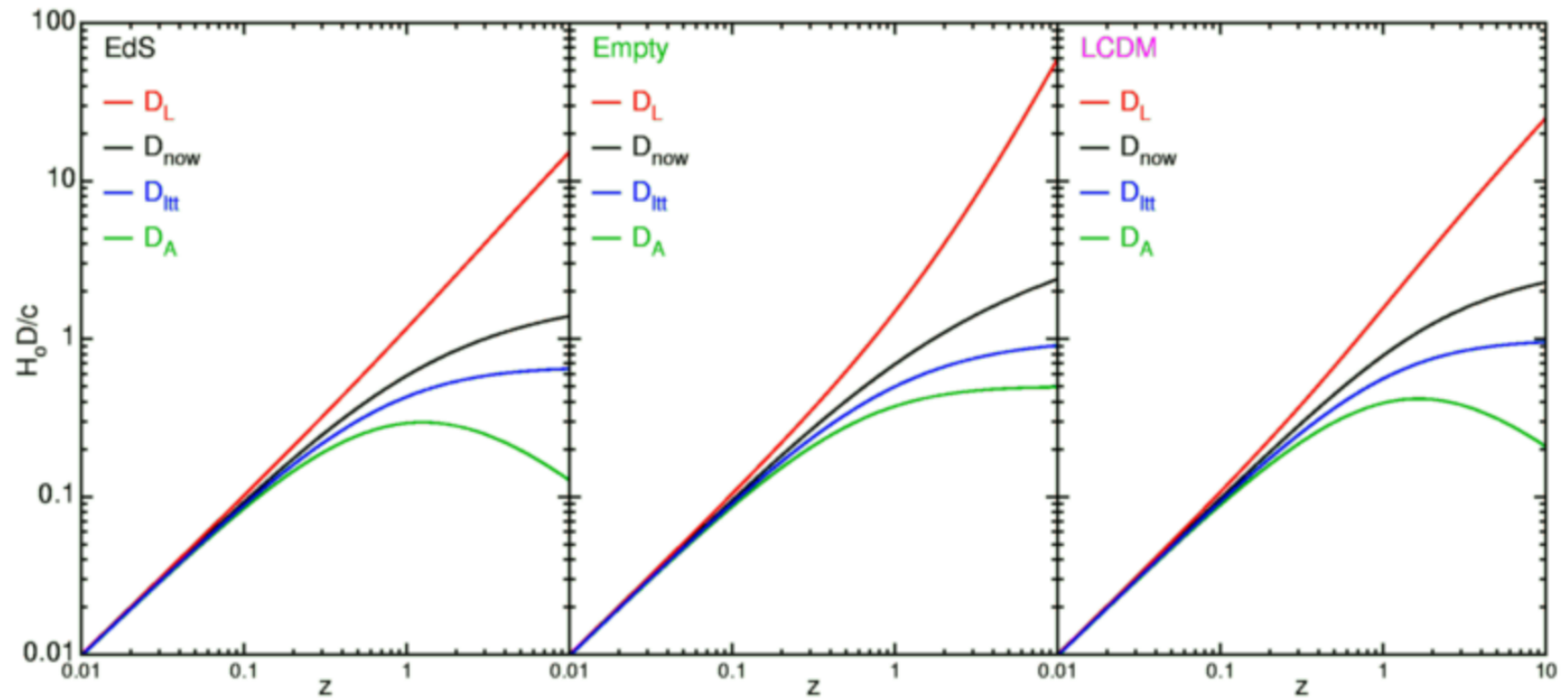
$$E(z) \equiv \sqrt{\Omega_M (1+z)^3 + \Omega_k (1+z)^2 + \Omega_\Lambda}$$

$$H_0 = 100 h \text{ km s}^{-1} \text{ Mpc}^{-1} \quad D_H \equiv \frac{c}{H_0} \quad D_C = D_H \int_0^z \frac{dz'}{E(z')}$$

$$D_M = \begin{cases} D_H \frac{1}{\sqrt{\Omega_k}} \sinh \left[\sqrt{\Omega_k} D_C / D_H \right] & \text{for } \Omega_k > 0 \\ D_C & \text{for } \Omega_k = 0 \\ D_H \frac{1}{\sqrt{|\Omega_k|}} \sin \left[\sqrt{|\Omega_k|} D_C / D_H \right] & \text{for } \Omega_k < 0 \end{cases}$$

$$D_L = (1+z) D_M$$

Luminosity distance and redshift



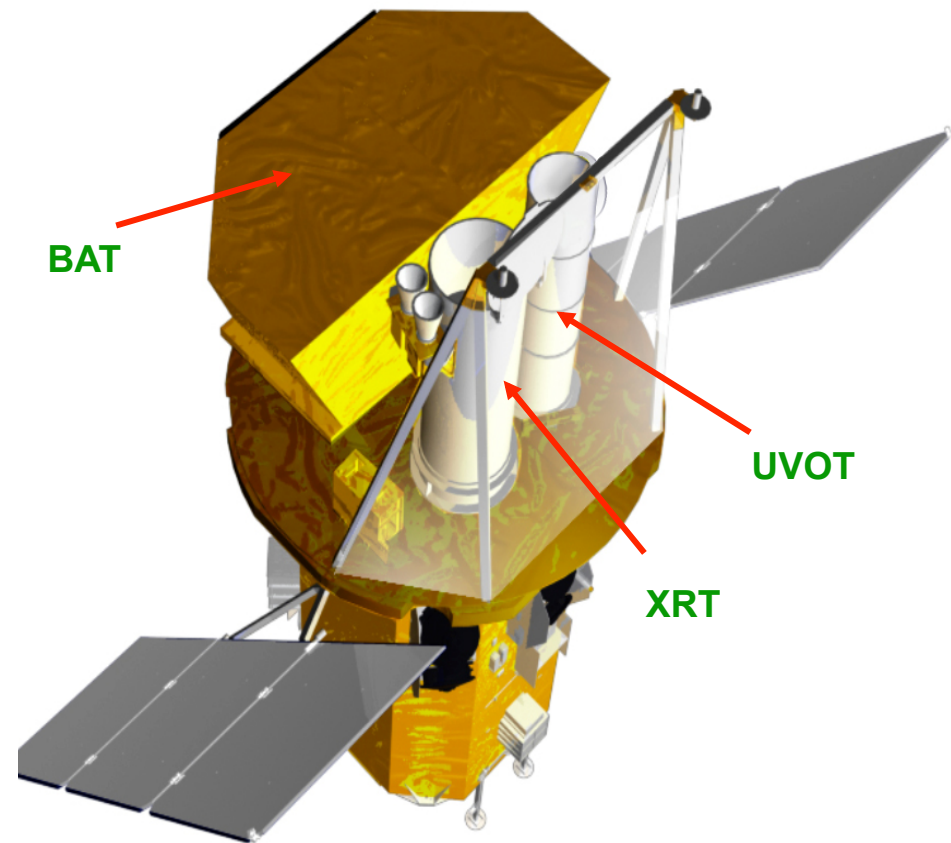
Swift Instruments

Instruments

- **Burst Alert Telescope (BAT)**
 - New CdZnTe detectors
 - Most sensitive gamma-ray imager ever
- **X-Ray Telescope (XRT)**
 - Arcsecond GRB positions
 - CCD spectroscopy
- **UV/Optical Telescope (UVOT)**
 - Sub-arcsec positions
 - Grism spectroscopy
 - 24th mag sensitivity (1000 sec)
 - Finding chart for other observers

Spacecraft

- Autonomous re-pointing, 20 - 75 s
- Onboard and ground triggers

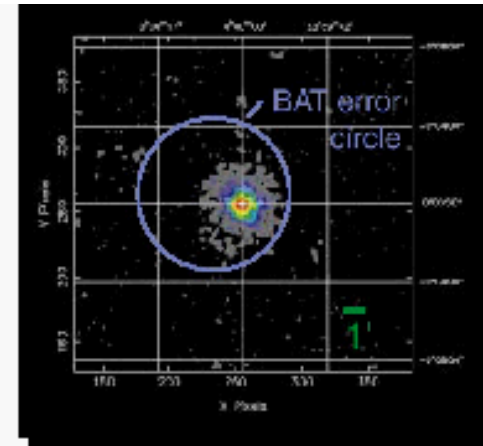
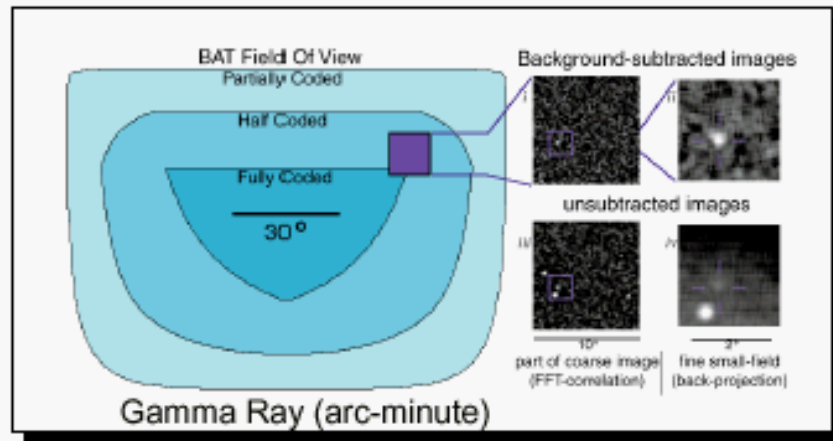


Swift

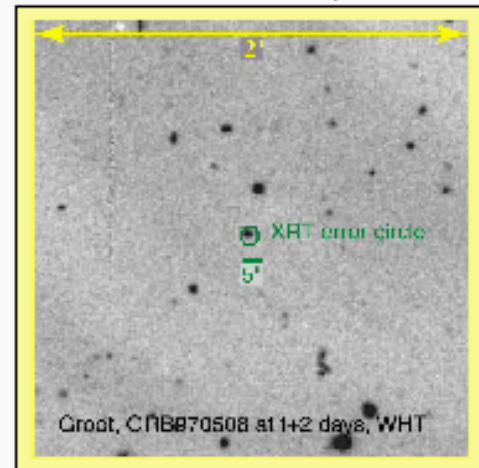
Details

- **BAT** (15-350 keV). Large (2 sr) field of view – detects bursts with arc min accuracy. And tells observers immediately.
- *Swift* automatically determines if it can view the GRB, and if so, slews to it.
- **XRT** (0.3-10 keV) and **UVOT** (~1000-6000 Å) begin observing typically within 100 s of the trigger.
- XRT can automatically detect afterglows, and downlinks limited data immediately. ~90% of BAT GRBs have promptly detected XRT afterglows.

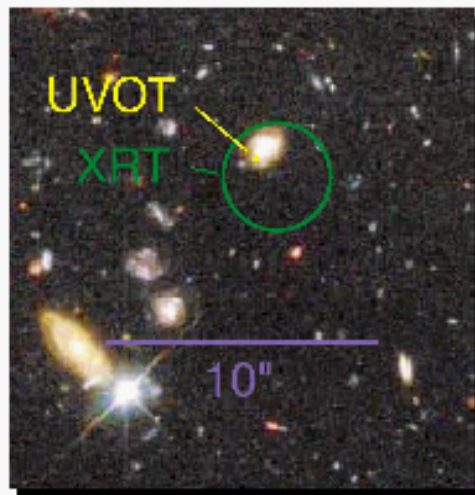
SWIFT



X-ray (2.5 arc-second)



HST, Keck, etc.



Exercise #3

- Check and navigate into Swift web sites
- Check the recently launched mission Einstein Probe
- Check what SVOM and Theseus missions will be ...

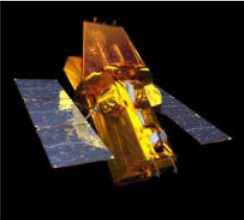
SWIFT

HEASARC Swift Home Archive Data Analysis Proposals & Tools Education & Public Outreach

Neil Gehrels Swift Observatory

About Swift Quicklook Data GCN Results Operations Related Sites Gallery

The Neil Gehrels Swift Observatory



Gamma-ray bursts (GRBs) are the most powerful explosions the Universe has seen since the Big Bang. They occur approximately once per day and are brief, but intense, flashes of gamma radiation. They come from all different directions of the sky and last from a few milliseconds to a few hundred seconds. So far scientists do not know what causes them. Do they signal the birth of a black hole in a massive stellar explosion? Are they the product of the collision of two neutron stars? Or is it some other exotic phenomenon that causes these bursts?

With Swift, a NASA mission with international participation, scientists

Swift Operations Status

All systems are operating normally.

Swift Resources

- » [GRB, BA, & TOO Contact Information](#)
- » [BAT Transient Lightcurves](#)
- » [Swift Supernovae](#)
- » [Observing Schedule](#)
- » [Journal Papers Related to Swift](#)
- » [Swift Press Release Image Archive](#)
- » [Swift User's Group \(SUG\)](#)
- » [Swift Mission Participants](#)

Latest Swift GRBs

- [GRB 220306B](#)

SWIFT

<https://www.swift.ac.uk/index.php>

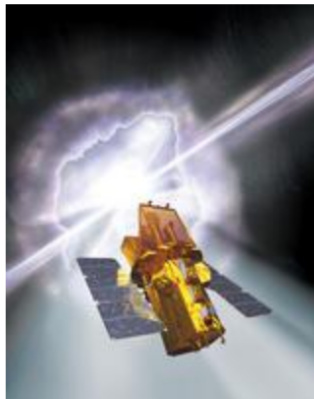


[Home](#) [About](#) [Support](#) [Data Access](#) [Data Analysis](#) [GRB Products](#) [Publications](#) [Links](#)

[site map](#) | Search: ?

The Neil Gehrels Swift Observatory

As of 3rd March, Swift has resumed normal science operations, with both ToO and GRB response re-enabled. High urgency ToOs can again be submitted. ([GCN 31668](#))



Picture courtesy of Spectrum Astro

Welcome to the UK Swift Science Data Centre.

The NASA-led Swift satellite discovers Gamma-Ray Bursts (GRBs) and measures their X-ray and optical afterglows to arc-second accuracy within a minute or two, continuing to make spectral observations until they fade from view days, weeks or even months later. Swift has been finding around 90 new bursts a year since launch in November 2004. It has provided the most complete study of GRBs so far, finding the most distant objects in the Universe and rapidly advancing science in this area. Swift is a rapid-response multi-wavelength facility which is ideal for observations of transient and variable sources; it has a Guest Investigator programme and a flexible Target of Opportunity programme which is well used.

On this site you can find out more about the mission and GRBs, as well as obtaining data from the on-board instruments and building X-ray products.

Latest Swift Detected GRBs

[GRB 220310C](#)
[GRB 220310A](#)
[GRB 220306B](#)
[GRB 220305A](#)
[GRB 220302A](#)

Quick Links

[Swift in the news](#)
[Training Opportunities](#)
[GRB and Swift Conferences](#)
[Targets of Opportunity](#)
[Guest Investigator Program](#)
[Build XRT products](#)

Helpdesk

Questions about Swift? Try our [guide to Swift](#) or the [guide to data processing and analysis](#). If these don't solve your problem, please feel free to [e-mail us](#) at swifthelp@le.ac.uk.

[List of acronyms and abbreviations](#)

We are located in the [Department of Physics & Astronomy](#), at the [University of Leicester](#) ([directions](#)).

One of our team is tweeting about life as a Swift scientist - [follow him on Twitter!](#)

SWIFT

<https://swift.asdc.asi.it/>



The screenshot shows the top section of the Space Science Data Center website. It features the SSDC logo on the left, the title "Space Science Data Center" in large orange letters in the center, and the ASI logo on the right. Below the title is a navigation menu with links for Home, About SSDC, News and Communication, Quick Look, Missions, Multimission Archive, Catalogs, Tools, Links, and Bibliographic services. There are also links for Helpdesk and Privacy, and social media icons for Facebook and Twitter. A banner below the menu shows a satellite and the text "Swift: Catching Gamma-Ray Bursts on the Fly". To the right of the banner are flags and links for the U.S., Italian, and U.K. sites. Below the banner is another navigation menu with links for Swift Home, About Swift, ASI HQ Swift Home, Swift Data Archive, Swift pointings, Swift Catalogs, Swift Quicklook Data, Swift Data Analysis, Swift Helpdesk, GCN, ToO Request Form, Malindi ground station, and Gallery.

The Swift Gamma-Ray Burst Mission

[ASI Swift Scientific Page \(Italian\)](#)

Swift is a MIDEX Gamma Ray Burst mission led by NASA with participation of Italy and the UK. The Swift data are available to the scientific community through data centers in the USA, Italy and the UK.

Italy contributes to the mission providing:

- The XRT X-ray mirror
- The Malindi ground station
- XRT data reduction and analysis software

The ASI Science Data Center (ASDC) contributes to the mission providing:

- [Swift Data Archive Mirror](#)
- [On-line XRT & UVOT data analysis](#)
- [Swift Quick Look Data \(XRT & UVOT Interactive Quick Look\)](#)
- XRT Burst Support (XBS) and Burst Advocate (BA) activity



An artist rendering of the Swift satellite catching a Gamma-ray Burst

High z - searches

High-z Universe: searching for the best probe

Galaxies

Pros

- ★ Multiband data are available (some)
- ★ Refurbished HST
- ★ Different technique (LBG/Ly α emission)
- ★ Do not “disappear”

Cons

- ★ Small region of the sky (11 arcmin²)
- ★ Required several hours of observations
- ★ Very faint objects
- ★ Galaxy templates are complex
- ★ Difficult determination of
Age/dust/SFR

Gamma-ray Bursts

Pros

- ★ Very bright
- ★ Happens everywhere
- ★ Can be followed quickly from space and ground (now at least)
- ★ **Have a very simple spectrum**
(synchrotron, simple power-law)
- ★ Allow better investigation of τ_{HI}

Cons

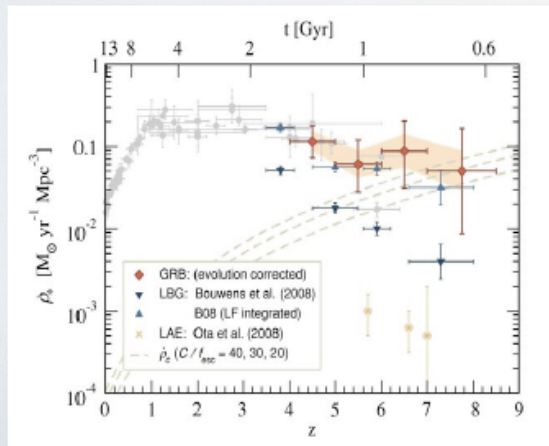
- ★ Rare (few “good ones”)
- ★ Fade fast, \sim minute position
identification (space mission)
- ★ Require multiband observations

High redshift GRB

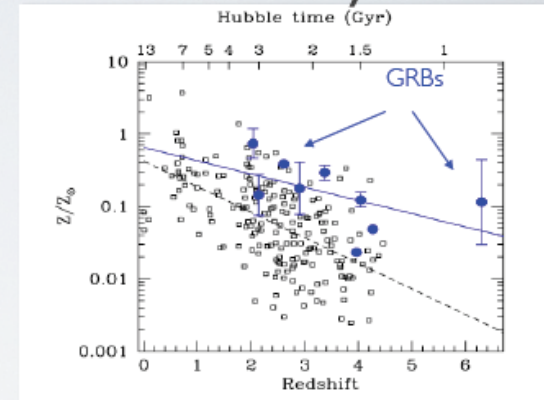
High-Redshift GRBs

z	GRB	Optical Brightness
9.4	090429B	K = 19 @ 3 hrs
8.2	090423	K = 20 @ 20 min
6.7	080813	K = 19 @ 10 min
6.29	050904	J = 18 @ 3 hrs
5.6	060927	I = 16 @ 2 min
5.3	050814	K = 18 @ 23 hrs
5.11	060522	R = 21 @ 1.5 hrs

Star Formation Rate



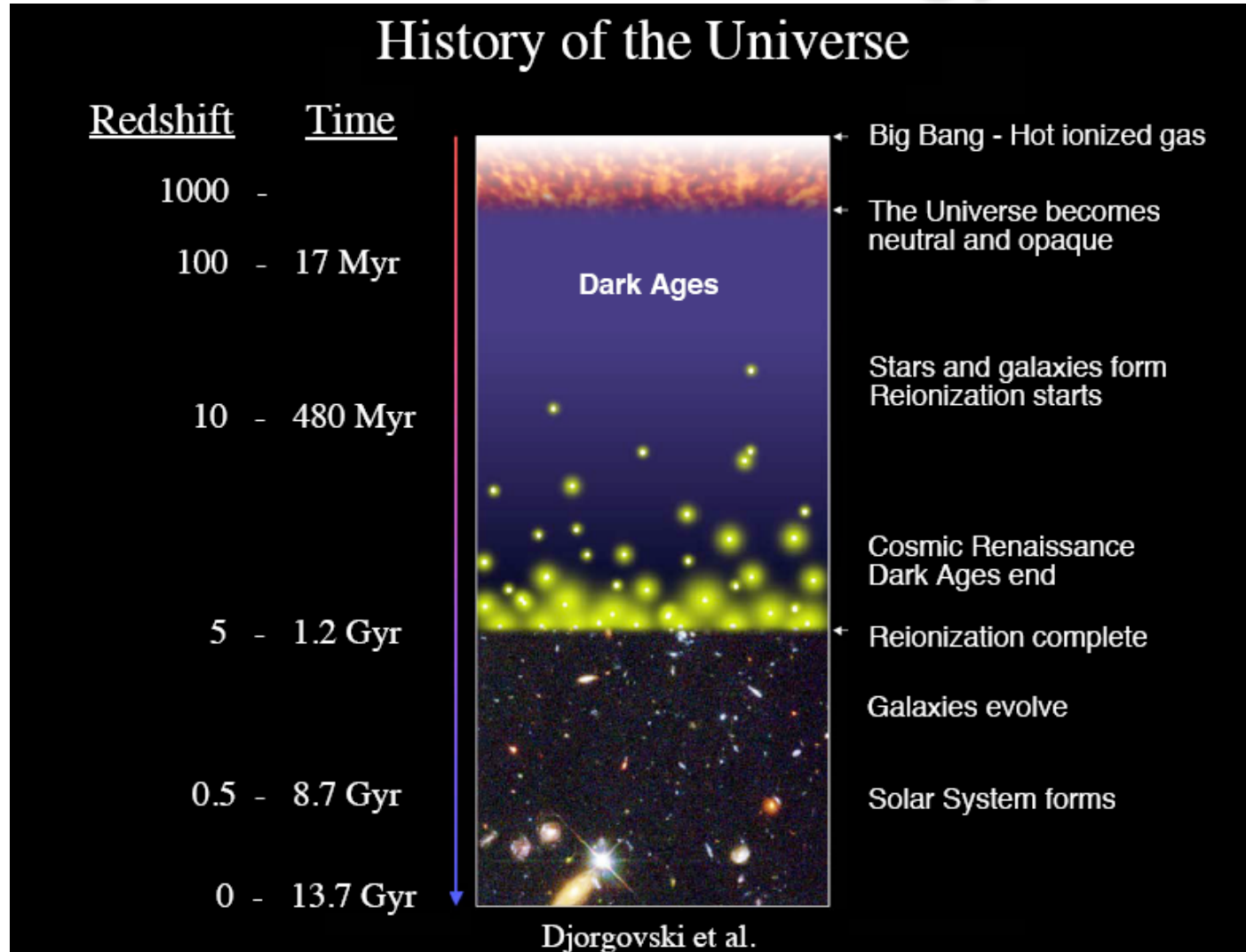
Metallicity



Savaglio 2006

Kistler et al. 2009;
Robertson & Ellis 2011

GRB & Cosmology



Einstein Probe

EINSTEIN PROBE IN A NUTSHELL

Einstein Probe is a mission led by the Chinese Academy of Sciences in collaboration with ESA and the Max Planck Institute for Extraterrestrial Physics.

In return for contributing to the mission's hardware and providing scientific advice, **ESA will get access to 10% of Einstein Probe's data.**



Hardware



Scientific advice



ESA's ground stations will be used to help download data from the spacecraft.



Launch

Einstein Probe will launch on a Chang Zheng (Long March) rocket from Xichang Satellite Launch Centre in China

Its expected lifetime is at least three years

Two science instruments

Wide-field X-ray Telescope (WXT): provides a large field of view and uses novel lobster-eye optics to observe a large portion of the sky at any given time

Follow-up X-ray Telescope (FXT): homes in on X-ray sources found with WXT with a much higher resolution and larger light-collecting power



Key questions

How common are **black holes**, how do they swallow matter, and what powers their jets?

What kind of events produce **gravitational waves**, and how?

What happens when a star explodes and goes **supernova**?

https://www.esa.int/ESA_Multimedia/Images/2023/12/Einstein_Probe_in_a_nutshell

Einstein Probe

Report of the first month of EP in-orbit commissioning phase

During the first month, the **satellite** has been confirmed to be in good condition.

- Basic satellite function testing has been completed.
- Attitude control stability and maneuvering speed meet the scientific requirements.
- Transmission of the links between the satellite and ground channels is stable.



Six of the twelve **WXT** modules have completed one week of bake-out, respectively.

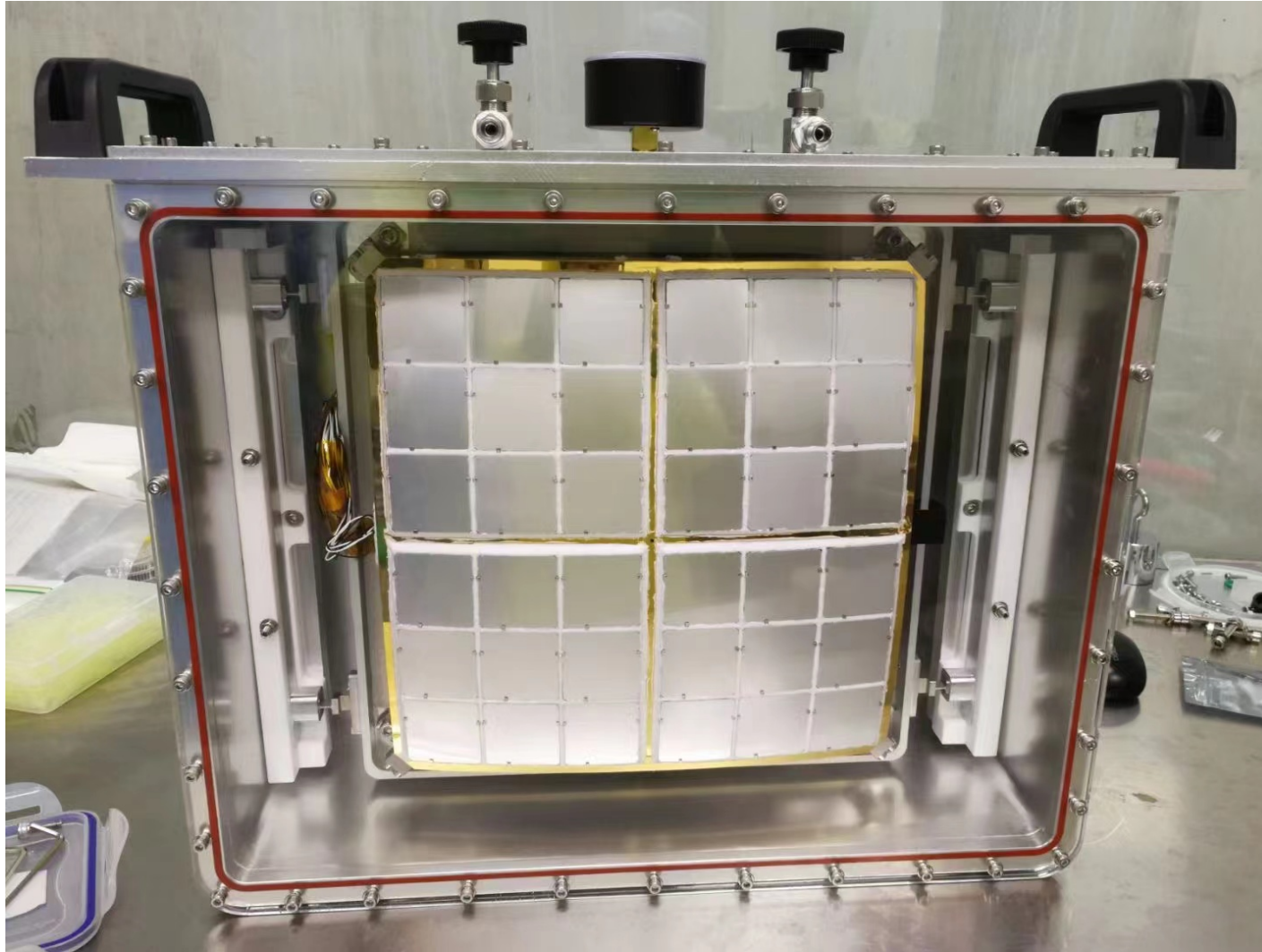
- Calibration observations are currently being conducted on the SNR Crab.
- Data from the calibration observations have been successfully transmitted to the ground.
- All levels of data products have been automatically produced.

The **FXT** payload has successfully completed the unlocking of the sunshield flipping mechanism.

- FXT refrigeration cooled the pn-CCD down to $-90\text{ }^{\circ}\text{C}$, and the pnCCD operated normally.
- Particle background data were collected with the telescope cover on.
- All levels of data products have been automatically produced.

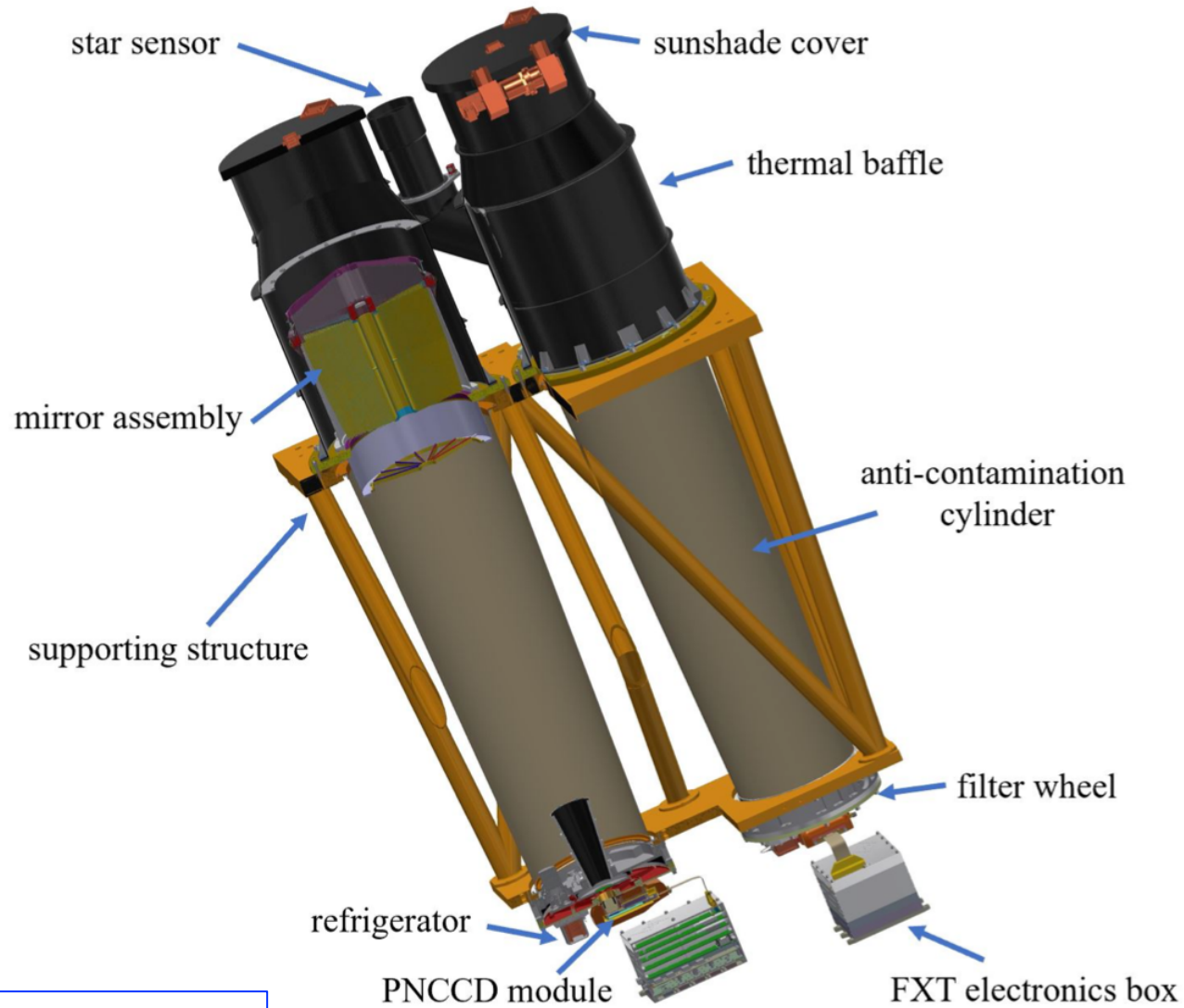
<https://ep.bao.ac.cn/ep/>

Einstein Probe



<https://ep.bao.ac.cn/ep/>

Einstein Probe



<https://ep.bao.ac.cn/ep/>

Einstein Probe

News

MORE



EP-WXT detected a fast X-ray transient EP240315a

[2024-03-17]

EP-WXT Detected a Bright X-ray Flare EP240305a

[2024-03-08]

EP-WXT Detected a Bright X-ray Flare in its Commissioning Phase

[2024-02-22]

EP Performs as Expected in the First Month of the In-orbit Commi...

[2024-02-09]



General Coordinates
Network

Missions Notices Circulars Documentation Sign in / Sign up

New Announcement Feature, Code of Conduct, Circular Revisions. See [news and announcements](#)

<https://ep.bao.ac.cn/ep/>

[← Back](#)

[Text](#)

[JSON](#)

[Cite \(ADS\)](#)

[Request Correction](#)

GCN Circular 35936

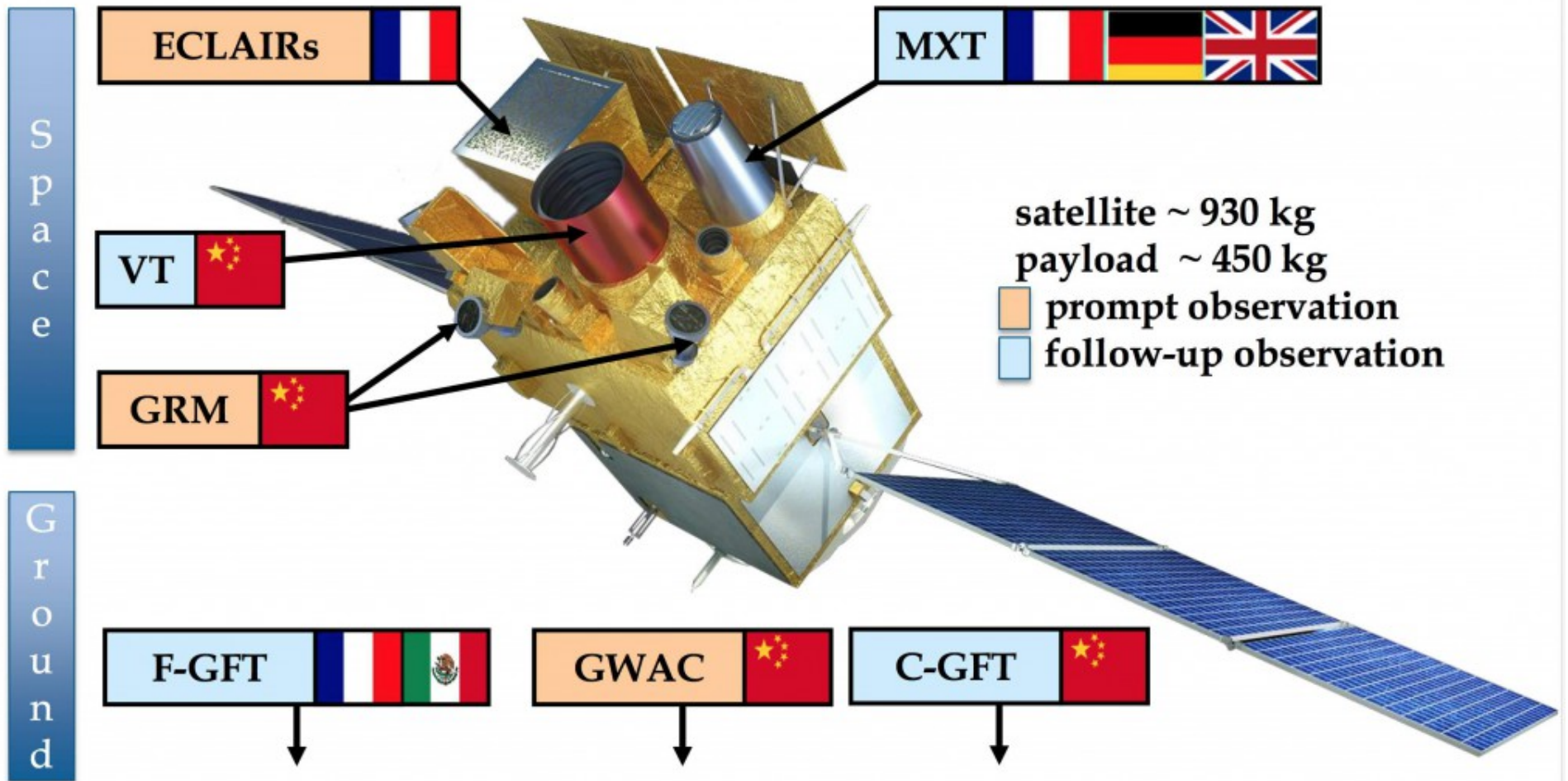
Subject X-ray transient EP240315a: VLT/X-shooter spectroscopic redshift of $z = 4.859$
Date 2024-03-17T06:54:26Z (13 hours ago)
From Andrea Saccardi at Observatoire de Paris <andrea.saccardi@obspm.fr>
Via Web form

A. Saccardi (GEPI/Obs. de Paris), A. J. Levan (Radboud Univ. & Warwick Univ.), Z. Zhu (NAOC), B. P. Gompertz (U. Birmingham), S. D. Vergani (GEPI/Obs. de Paris & IAP & INAF/OABr), G. Pugliese (API), D. Xu (NAOC), D. B. Malesani (DAWN/NBI and Radboud Univ.), report on behalf of the Stargate collaboration:

We observed the field of the ATLAS optical counterpart [AT2024eju](#) (Srivastav et al., GCN [35932](#)) of the fast X-ray transient EP240315a reported by the WXT instrument during the commissioning phase of the Einstein Probe mission (Zhang et al, GCN [35931](#)) using the ESO/VLT UT3 (Melipal) equipped with the X-shooter spectrograph. Our spectra cover the wavelength range 3000–21000 Å, and consist of 4 exposures of 1200 s each. Observations started at 01:02:52 UT on Mar 17 2024 (~29 hr after the trigger). We detect a clear continuum across both VIS and NIR arms. From the detection of a Ly α absorption at ~7120 Å and multiple absorption features, which we interpret as being due to OI, SiII, NV, CIV and SiIV, we infer a redshift of $z = 4.859$. We also note the presence of additional absorption features likely due to multiple intervening systems. The high redshift of the transient suggests a highly energetic event and potentially links this Fast X-ray Transient to a GRB-like phenomena.

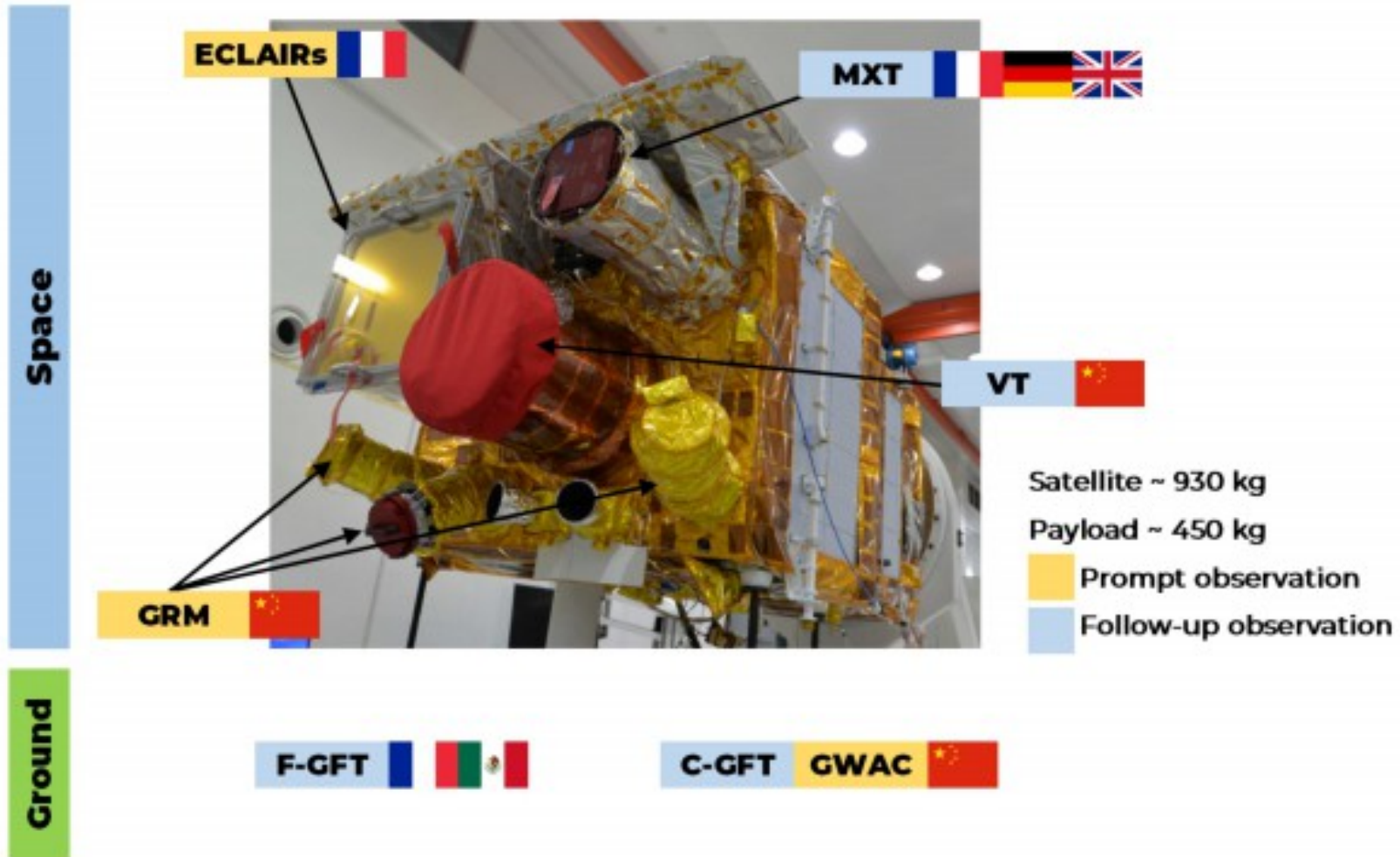
We acknowledge the excellent support from the ESO staff in Paranal, in particular Joe Anderson and Matias Jones.

SVOM



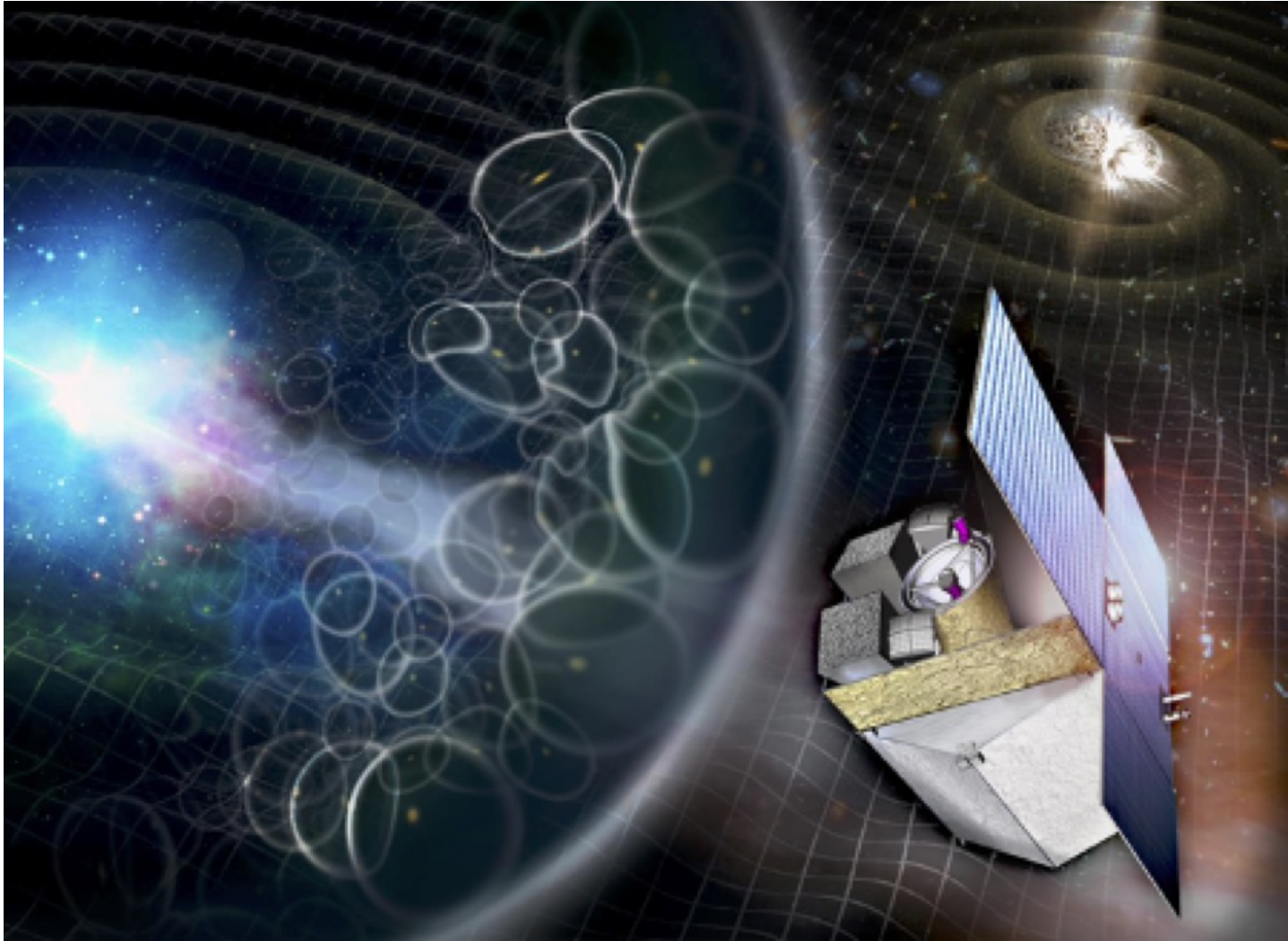
<https://www.svom.eu/en/the-svom-mission/>

SVOM



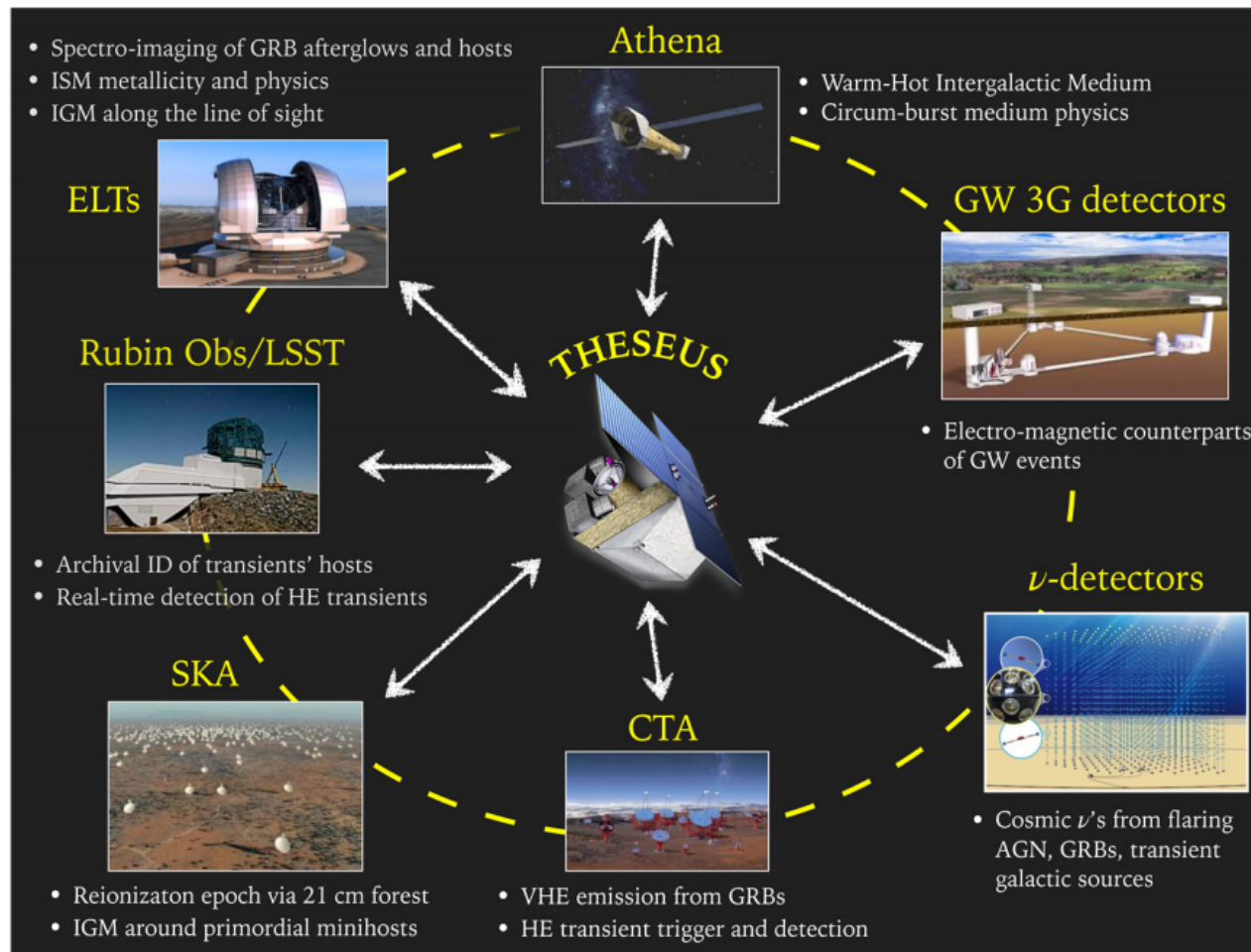
<https://www.svom.eu/en/the-svom-mission/>

THESEUS



https://sci.esa.int/documents/34375/36249/Theseus_YB_final.pdf

THESEUS

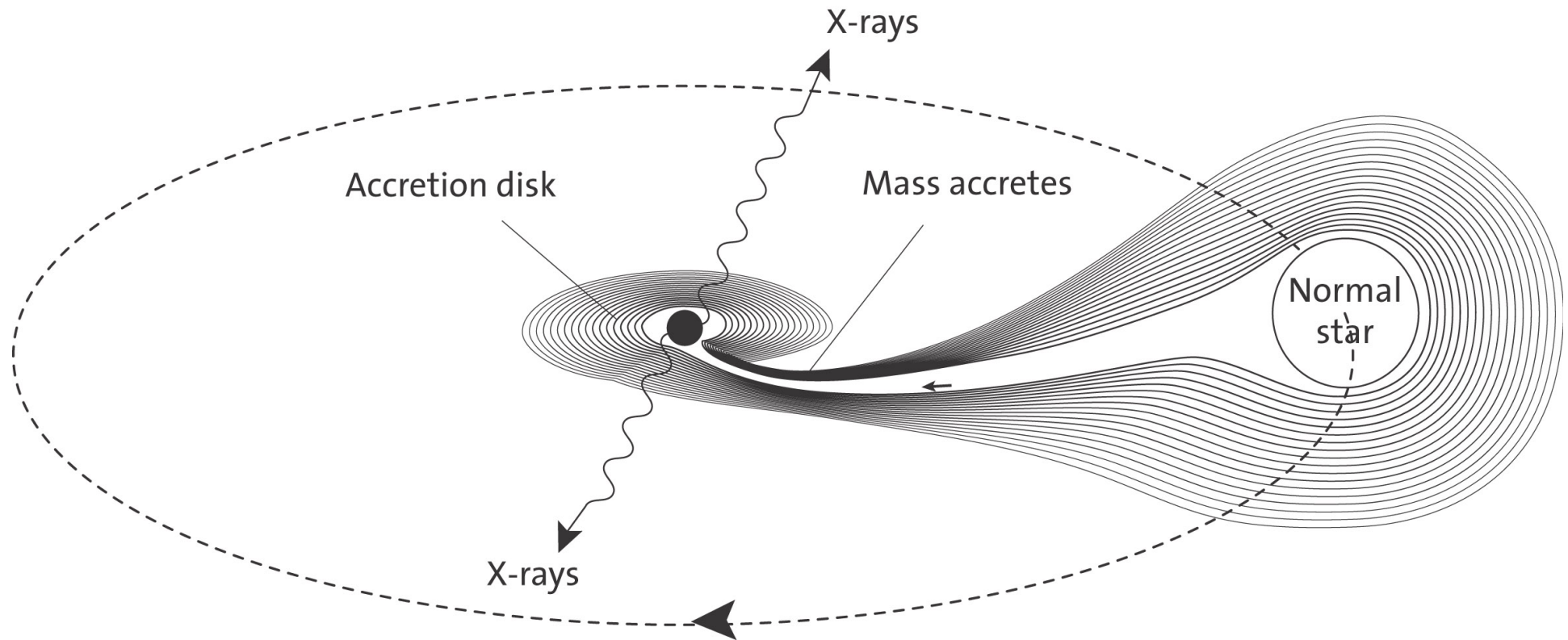


https://sci.esa.int/documents/34375/36249/Theseus_YB_final.pdf

Astrofisica Nucleare e Subnucleare

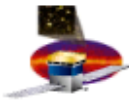
“X-ray” Astrophysics

Nobel prize 2002 – R.Giacconi



“ ... for pioneering contributions to astrophysics,
which have led to the discovery of cosmic X-ray sources”

Detector Project



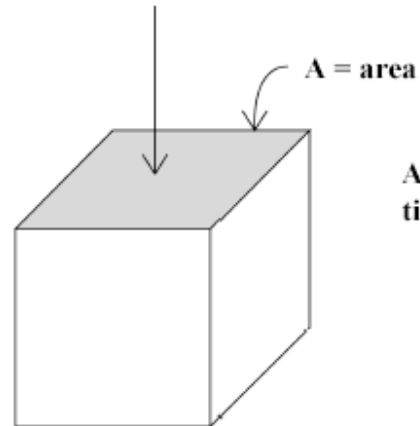
GLAST Project

For SWG discussion , Huntsville, 2002.9.13

Definition of Terms

- ◆ Effective Area:

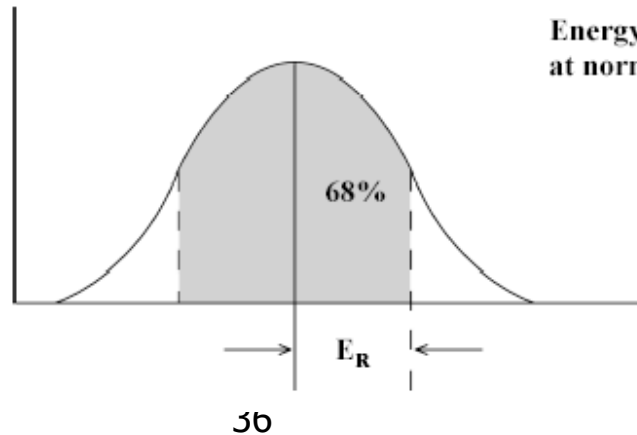
A_{eff}



Area at normal incidence
times detection efficiency.

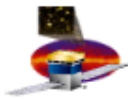
- ◆ Energy Resolution:

E_R



Energy 68% spread
at normal incidence.

Detector Project



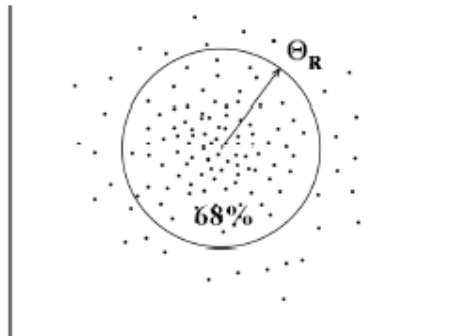
GLAST Project

For SWG discussion, Huntsville, 2002.9.13

Definition of Terms

- ◆ Angular Resolution:

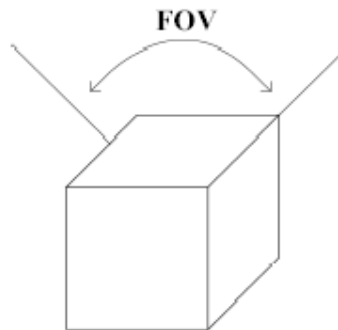
Θ_R



Space angle for 68% containment at normal incidence.

- ◆ Field of View:

FOV



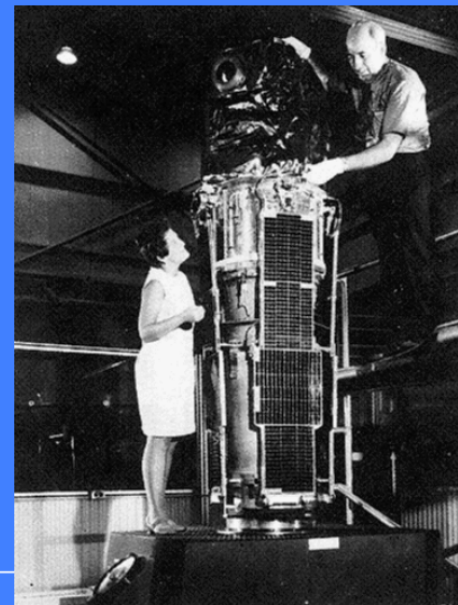
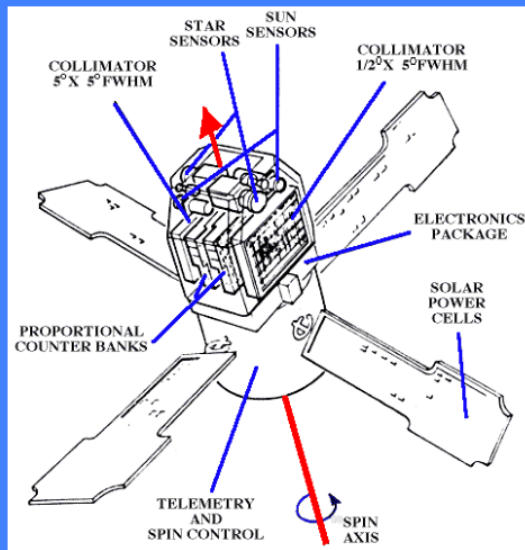
Integral effective area over solid angle divided by peak effective area.

- ◆ Sensitivity:

Flux of weakest source that can be detected at 5 sigma significance.

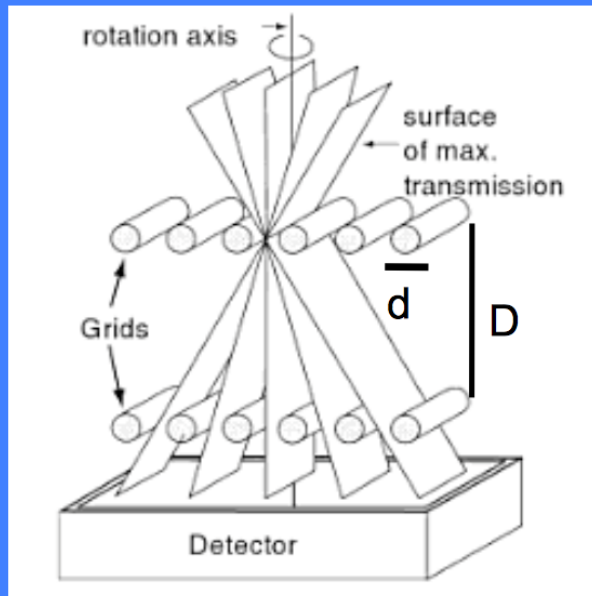
Scanning with Slat Collimators

- **Imaging the sky with non-imaging X-ray instruments as a goal**
- **Linear scanning means position is determined in one direction**
- **At least a second scanning, preferentially in the direction perpendicular to the previous one**
- **First all-sky survey in X-rays by Uhuru (1970-72): 2 prop. counters with metal collimators ($0.5^\circ \times 5^\circ$, $5^\circ \times 5^\circ$ FWHM)**

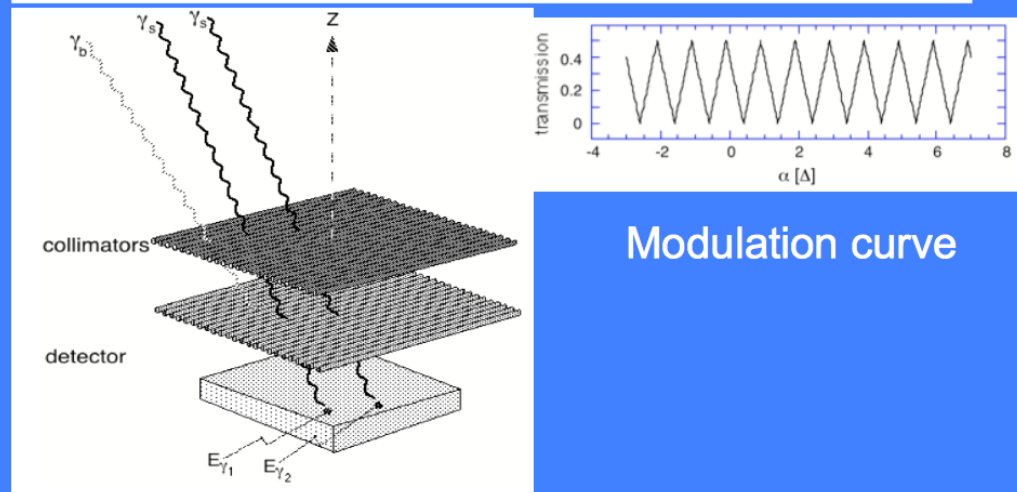


Scanning Grid Collimators

- Two or more plane (“grid” of absorbing rods) collimators to improve angular resolution
- Higher resolution with three or more grids (e.g., 4 in HEAO-1 A-3 experiment)
- Two-dimensional measurements need scans in two or more directions



Double-grid collimator
Transmission Function of triangular shape
Angular resolution: d/D



Modulation curve

Sensibilità - 1

- **Sensibilità = flusso minimo rivelabile**
 - **Emissione nel continuo:** fotoni $\text{cm}^{-2} \text{s}^{-1} \text{keV}^{-1}$
 - **Emissione di righe:** fotoni $\text{cm}^{-2} \text{s}^{-1}$
- **C_S = Tasso di conteggi di sorgente**
- **C_{Bkg} = Tasso di conteggi di fondo**
assumendo una statistica poissoniana

$$SNR = n_\sigma = \frac{C_S}{\sqrt{C_S + C_{Bkg}}}$$

In realta' quello che si misura e' $(S+B)-B$ in un dato intervallo di tempo

$$\begin{aligned} S &= (S + B) - B \longrightarrow \sigma_S^2 = \sigma_{S+B}^2 + \sigma_B^2 = \\ &= (\sqrt{(S + B)})^2 + (\sqrt{B})^2 = S + B + B = S + 2B \\ SNR &= S / \sigma_S = S / \sqrt{(S + 2B)} \end{aligned}$$

Sensibilità – 2 – “basic” dependencies

$$S = \varepsilon A T \Delta E F_{src}$$

$$B = A T \Delta E F_{bkg}$$

ε =efficienza di rivelazione fotoni della sorgente
 A =area efficace
 T =tempo di esposizione
 ΔE =banda energetica
 F_{src} =flusso della sorgente
 F_{bkg} =fondo strumentale

$$B \ll \varepsilon F_{src}$$

$$SNR = \frac{S}{\sqrt{S + 2B}} \approx \sqrt{S} \propto \sqrt{F_{src} T}$$

the source dominates the signal

$$B \gg \varepsilon F_{src}$$

$$SNR = \frac{S}{\sqrt{S + 2B}} \approx S / \sqrt{2B} \propto \sqrt{T} (F_{src} / \sqrt{2F_{bkg}})$$

Backg-dominated obsn.



$$SNR = n_{\sigma} \approx \frac{\varepsilon \cdot A \cdot T \cdot \Delta E \cdot F}{\sqrt{A \cdot T \cdot \Delta E \cdot B}} \rightarrow F_{Min} = \frac{n_{\sigma}}{\varepsilon} \sqrt{\frac{B}{A \cdot T \cdot \Delta E}}$$

to give an idea of the main dependencies of the limiting flux (sensitivity)

In the “real world”, the background is not only instrumental but also cosmic

S=source flux density [counts/m² s]

A=area of the detector

Ω=solid angle subtended by the beam of the telescope on the sky

B₁=instrumental (particle) background [counts/s]

B₂=cosmic background (XRB) [phot/m² s ster]

T=exposure time

SOURCE=S×A×T (photons related to the source)

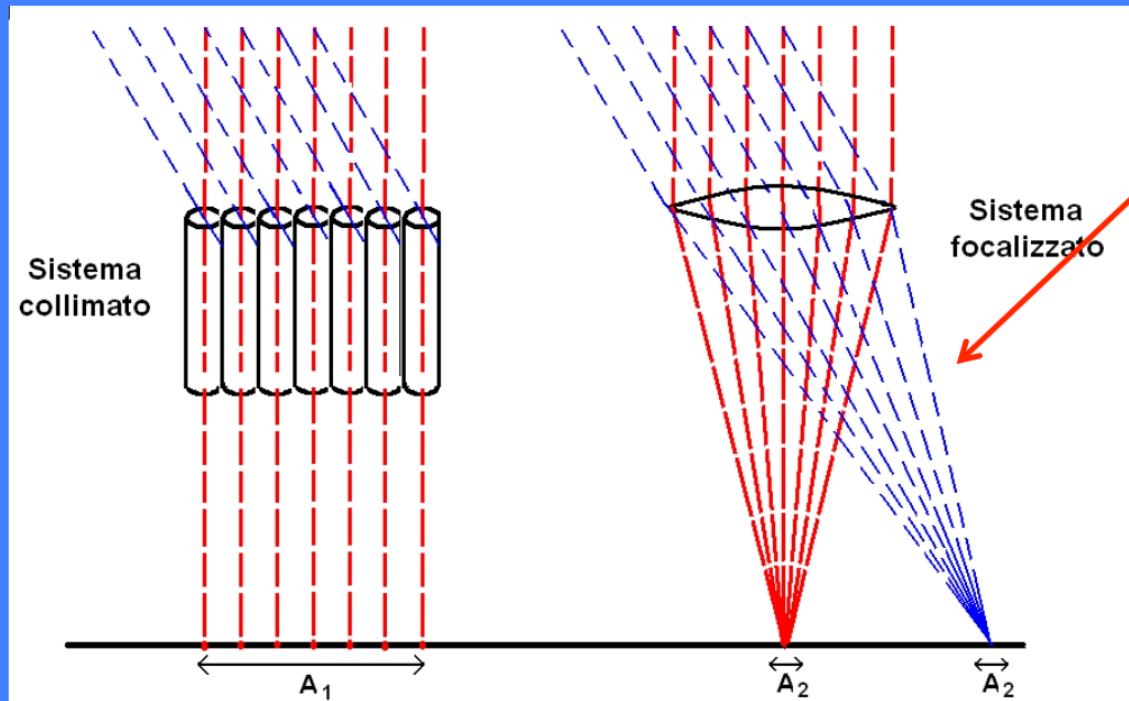
BACKGROUND=B₁×T + B₂×A×Ω×T (photons related to the backgrounds)

$$N = \sqrt{(B_1 + B_2 A \Omega) \times T}$$

$$S/N = \frac{SAT}{\sqrt{(B_1 + B_2 A \Omega) \times T}} = \frac{SA^{1/2}T^{1/2}}{\sqrt{\left(\frac{B_1}{A}\right) + \Omega B_2}}$$

$$S/N = 5 \Rightarrow S_{\min} = 5 \sqrt{\frac{B_1 / A + \Omega B_2}{AT}}$$

Focalizzazione vs collimazione



Proper imaging of X-rays below 20-40 keV

A_d = PSF projected on the focal plane

$$F_{\min} \approx n_{\sigma} \frac{\sqrt{2B}}{\sqrt{A_{\text{det}} T_{\text{int}} \Delta E}}$$

$$F_{\min} \approx n_{\sigma} \frac{\sqrt{BA_d}}{A_{\text{eff}} \sqrt{T_{\text{int}} \Delta E}}$$

Sistema collimato: limita la regione di cielo da cui puo' provenire un segnale, (quindi limita il background), non incrementandone la "densita"

Sistema focalizzato: fa corrispondere ad ogni sorgente un punto nel piano focale, e "concentra" il segnale, producendo un'immagine

$$C_B = B A_d \Delta E \Delta t$$

Background counts from a collimated telescope with detector area A_d , sensitive over the band ΔE , in a time interval Δt

$$\sigma(C_B) = C_B^{1/2}$$

The counts obey the Poisson statistics

$$C_S = S_E A_d \Delta E \Delta t \eta_E$$

Source counts collected from a source with flux S_E in the same conditions ($QE = \eta_E$)

$$C_{\text{meas}} = (C_S + C_B) - C_B$$

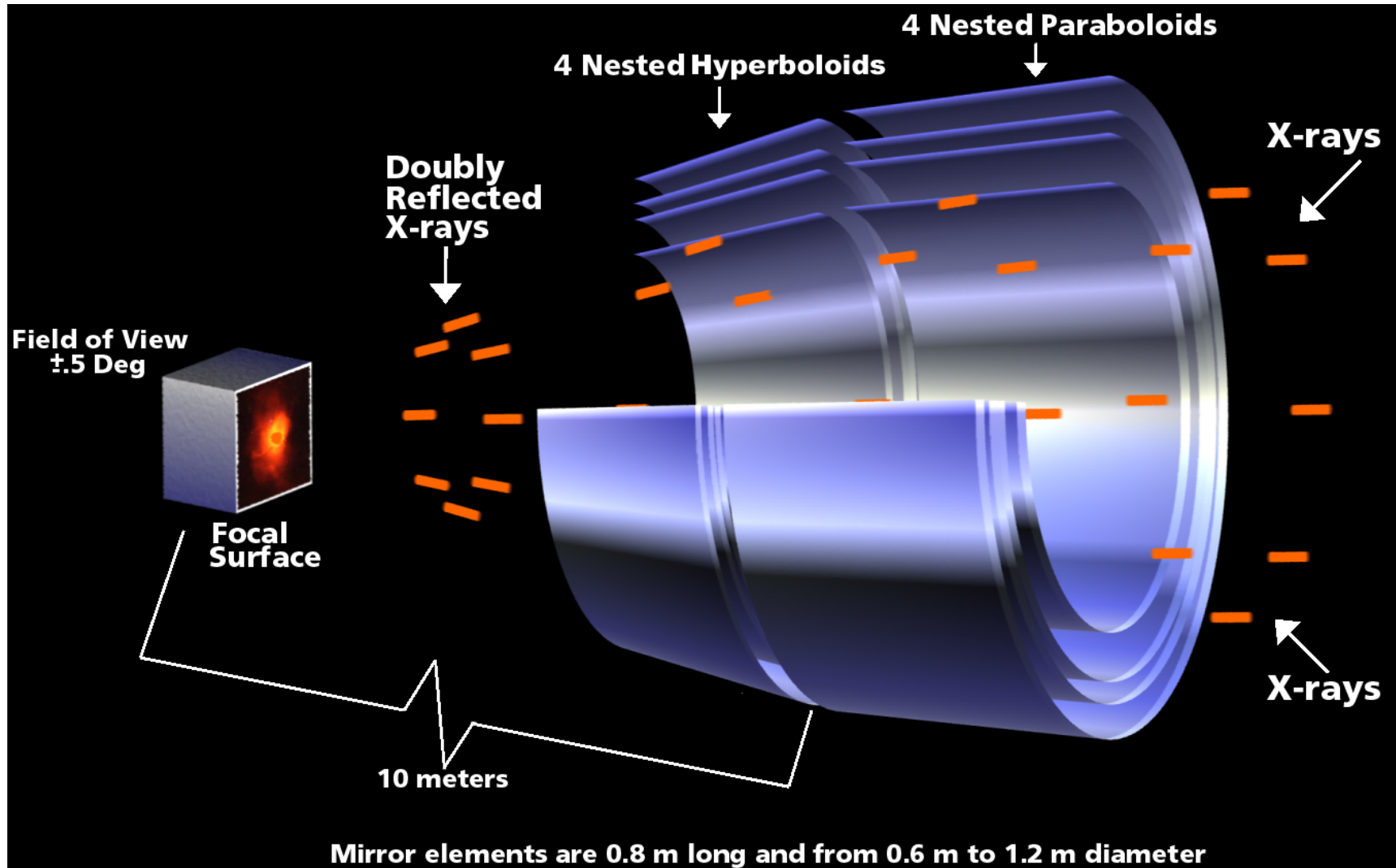
Measured counts (backg-subtracted)

$$\sigma^2(C_{\text{meas}}) = 2\sigma^2(C_B)$$

Background dominates fluctuations

$$S/N = n_\sigma = \frac{C_S}{\sqrt{2C_B}} = \frac{S_E A_d \Delta E \Delta t \eta_E}{\sqrt{2B A_d \Delta E \Delta t}}$$
$$S_{E,\text{min}} = \frac{n_\sigma \sqrt{2B}}{\eta_E \sqrt{A_d \Delta t \Delta E}}$$

X-Ray Mirrors



Why do we use X-ray optics

- To achieve the best 2-dim angular resolution
 - To distinguish nearby sources or different regions of the same source
 - To perform morphological studies
- As a collector to “gather” weak fluxes (case of limited photon statistics)
- As a concentrator, so that the image photons may interact in a small region of the detector, thus limiting the influence of the background
- To serve with high spectral resolution dispersive spectrometers such as transmission or reflection gratings
- To simultaneously measure both the source(s) of interest and the contaminating background in other (source-free) regions of the detector

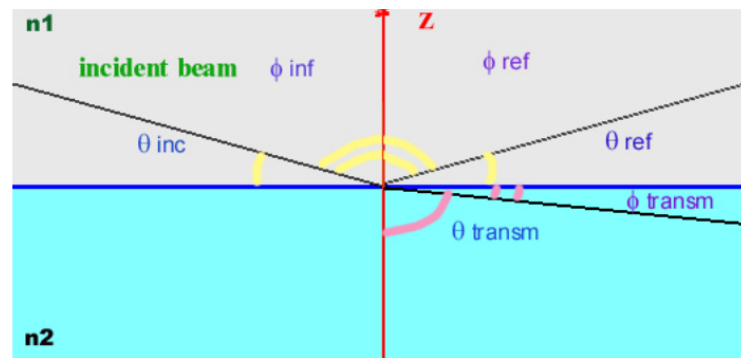
X-ray optical constants

- X-rays are hard to refract or reflect: the refractive index of all materials in X-rays is very close to 1 and only slightly less than 1 → X-rays are above the characteristic energy of bonded e⁻ in atoms
- complex index of refraction of the reflector to describe the interaction X-rays /matter (see, for a review, Aschembach et al. 1985, Rep. Prog. Phys. 48, 579)

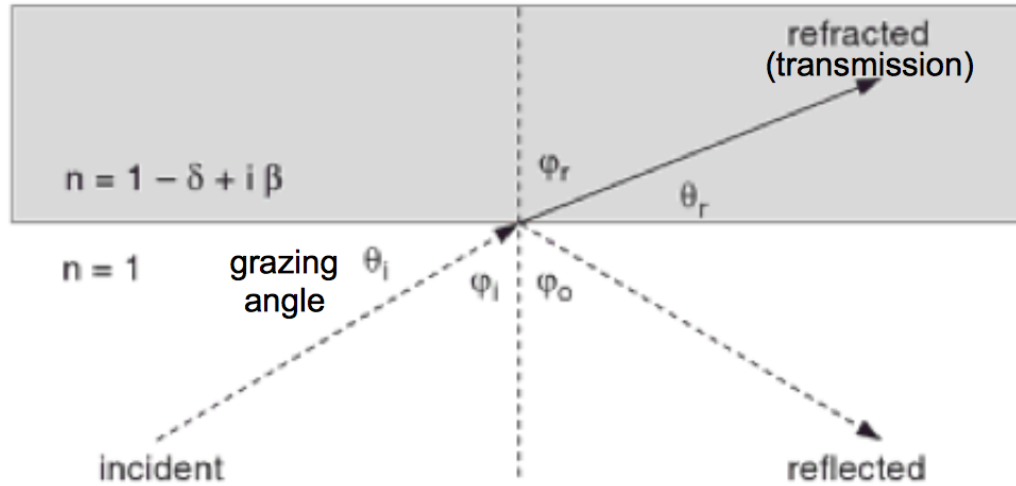
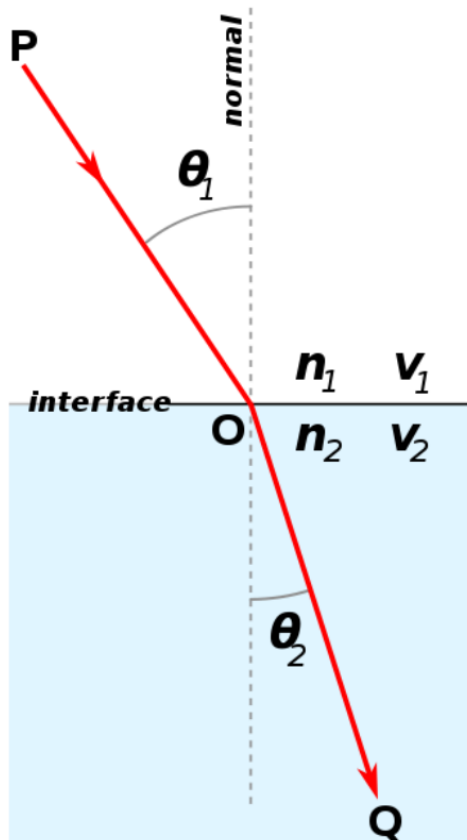
$$n=1-\delta+i\beta$$

where δ describes the phase change and
 β accounts for the absorption

δ and β depend on the wavelength

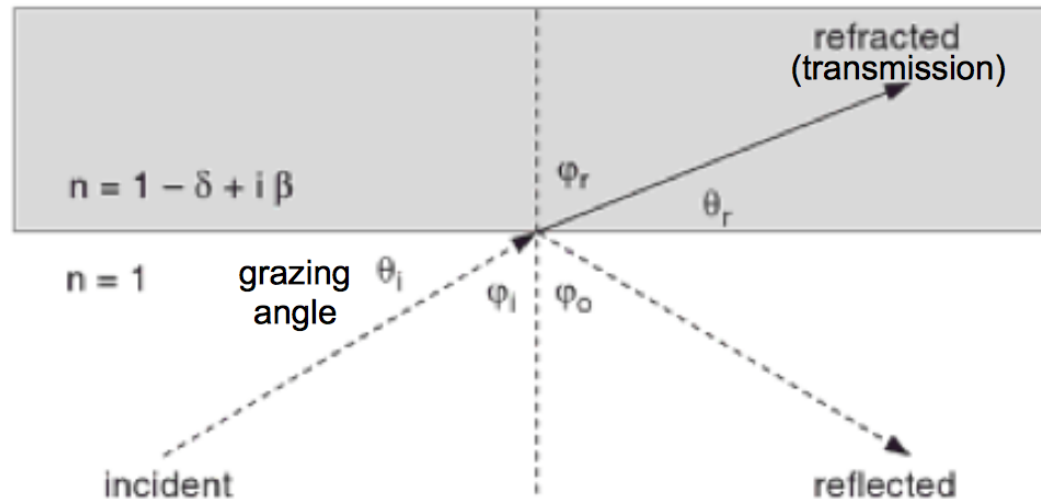


- the amplitude of reflection is described by the Fresnel's equations



Snell's Law of Refraction:
relationship between the angles of incidence
and refraction in a medium

$$n_1 \sin \theta_1 = n_2 \sin \theta_2$$



$$n_1 = 1, n_2 = (1 - \delta) \rightarrow \sin \phi_i = (1 - \delta) \sin \phi_r$$

$$\vartheta = (\pi / 2) - \phi$$

$$\cos(90 - \phi_i) = \cos \vartheta_i = (1 - \delta) \cos(90 - \phi_r) = (1 - \delta) \cos \vartheta_r$$

$$\Rightarrow \cos \vartheta_i = \cos \vartheta_r (1 - \delta)$$

Total reflection if no real solution for ϑ_r
 $\delta > 0, \cos \theta_r \leq 1 \rightarrow$ There is a **critical angle** θ_c below which refraction is impossible
 and total external reflection occurs (grazing angle, $\theta_i = \theta_c$)



Extreme case for
low θ_r values

$$1 = \cos \vartheta_r = \cos \vartheta_c / (1 - \delta) \rightarrow \cos \vartheta_c = 1 - \delta$$

Total X-ray reflection at grazing incidence

- Real part of n slightly less than unity for matter at X-rays, =1 in vacuum (total external reflection); $\delta \ll 1$

- Snell's law ($n_1 \cos\theta_1 = n_2 \cos\theta_2$) to find a critical angle for total reflection

- (Total) external reflection in vacuum for angles $<$ critical angle: $\cos\theta_{crit} = 1 - \delta$

- X-ray partially reflected also for $\theta > \theta_{crit}$; also, some absorption in the material

- $\cos(\theta_{crit}) = 1 - \theta_{crit}^2/2 = 1 - \delta \xrightarrow{\text{low angles}} \theta_{crit} = \sqrt{2\delta}$

- Far from fluorescent edges:

$$\delta \approx \frac{N_0 Z r_e \rho \lambda^2}{2\pi A}$$

where N_0 =Avogadro's number

Z =atomic number

r_e =electron radius

ρ =density

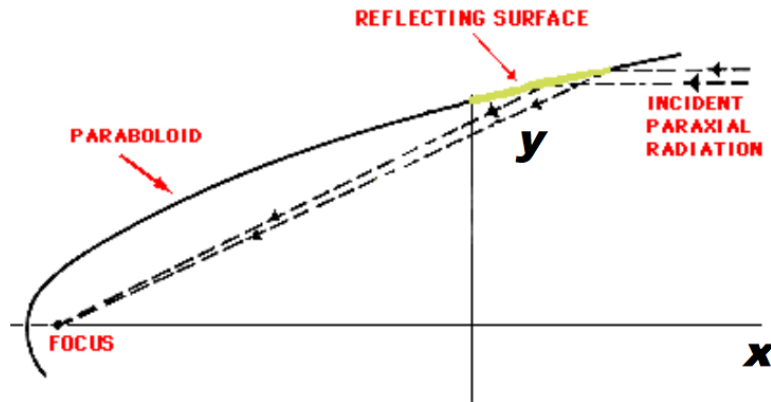
λ =wavelength of the incoming photon

A =atomic weight

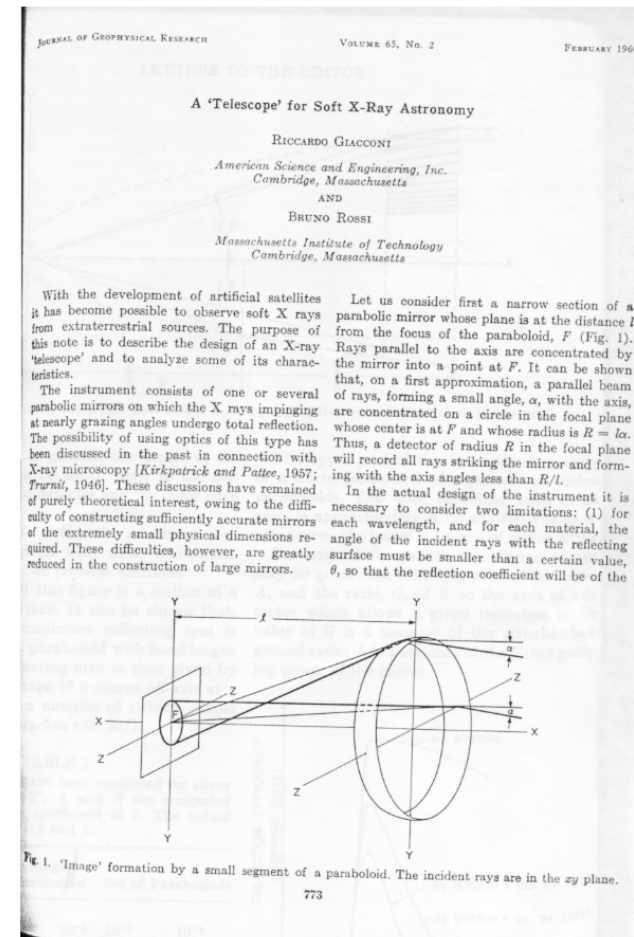
Critical angle:

- Inversely dependent on energy
- Higher Z materials reflect higher energies, for a fixed grazing angle
- Higher Z materials have a larger critical angle at any energy

X-ray mirrors with parabolic profile

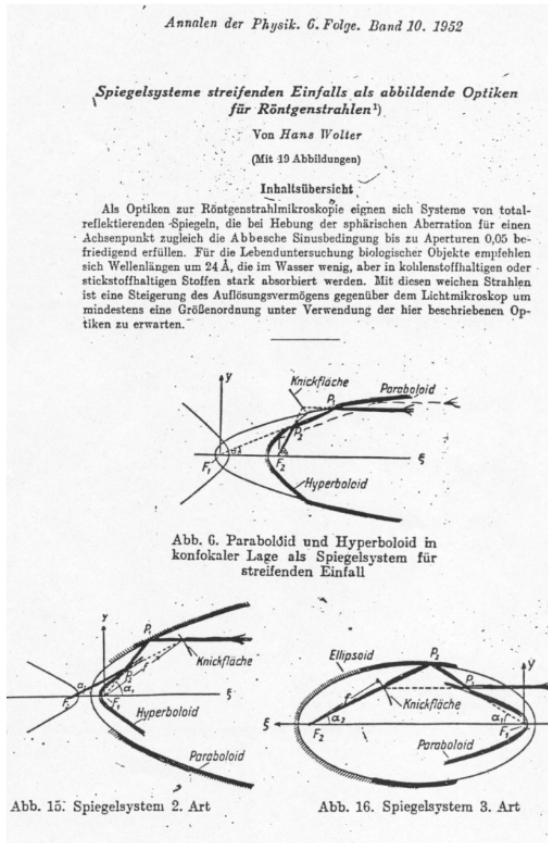


- perfect on-axis focusing
- off-axis images strongly affected by coma

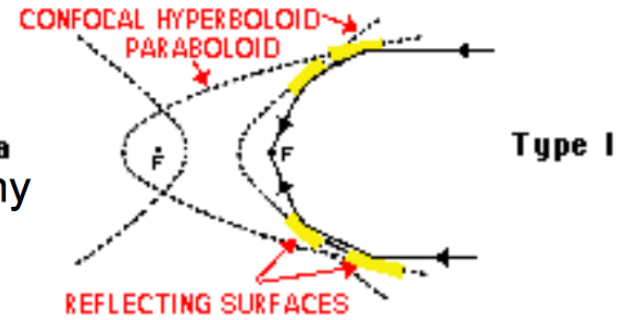


Wolter, 1952

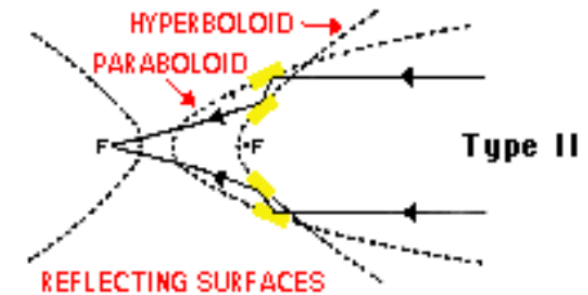
Wolter's solution to the X-ray imaging



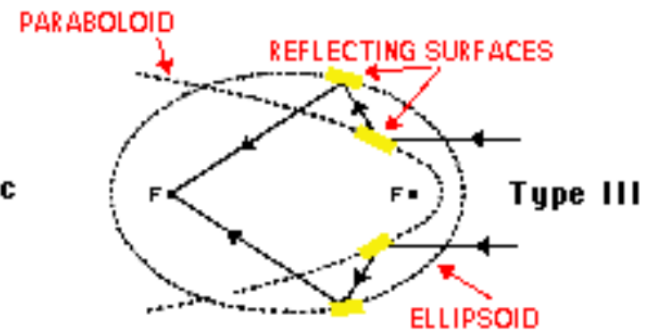
Fine for **a**
X-ray astronomy



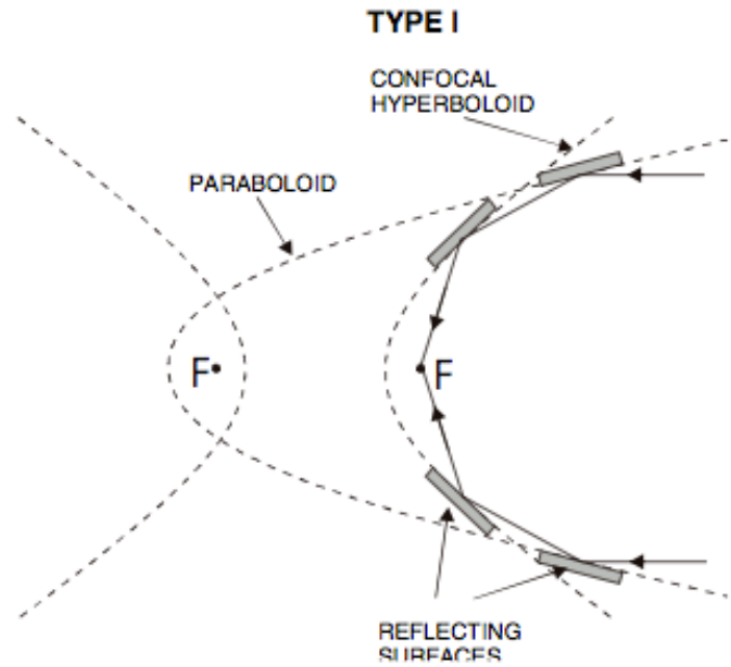
Applied in solar **b**
X-ray telescopes



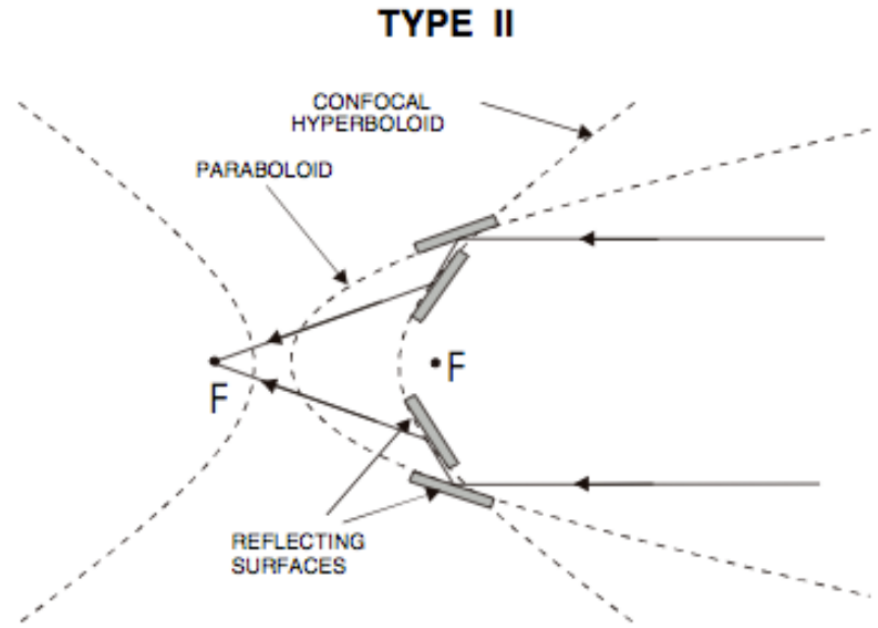
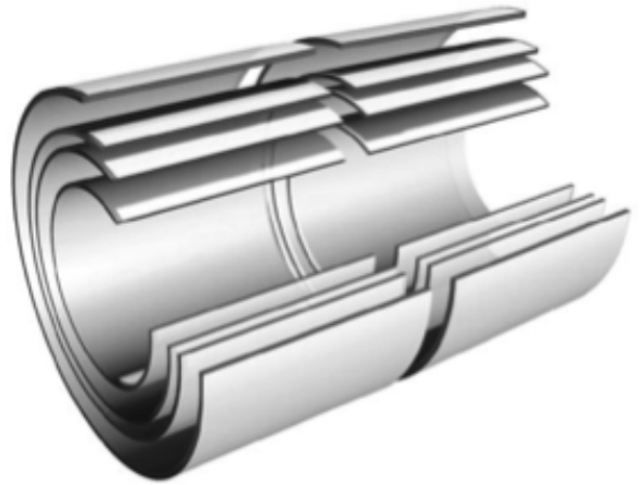
Not adopted **c**



H. Wolter, Ann. Der Phys., NY10, 94 (1952)

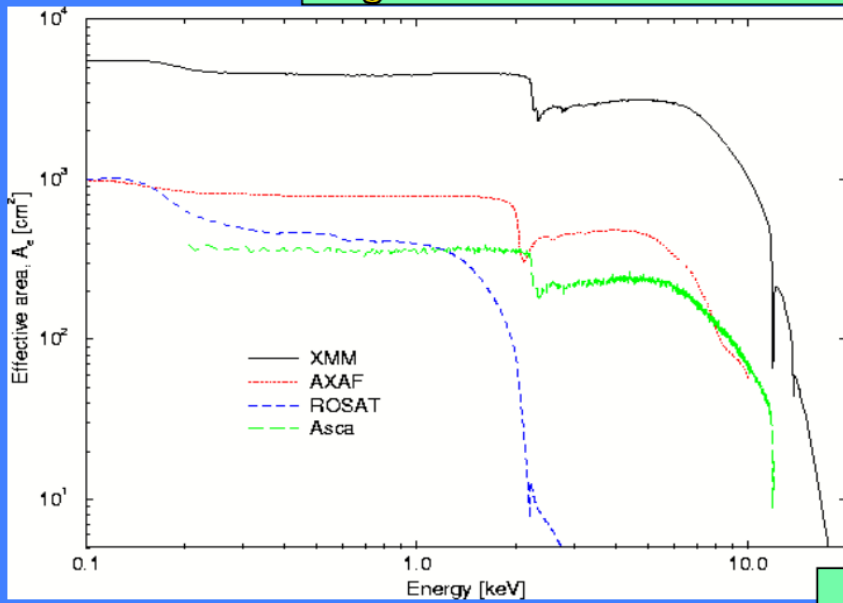


Wolter-I optics
Paraboloid → Hyperboloid

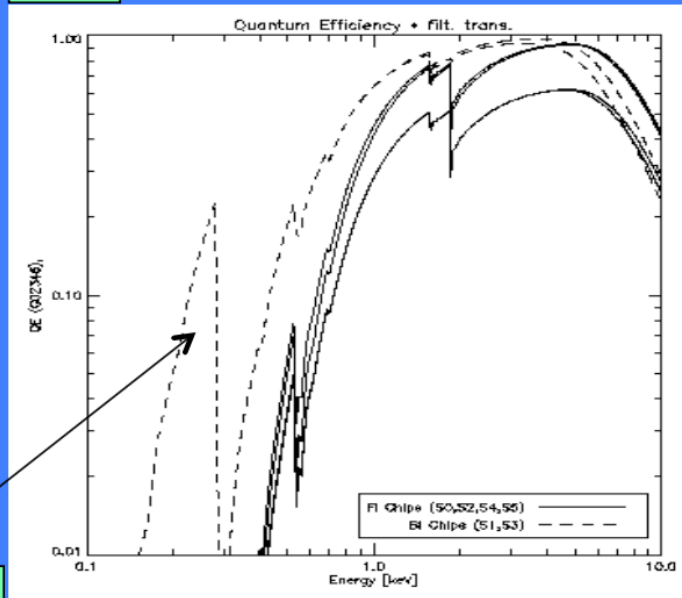


Wolter-II optics
Paraboloid → Hyperboloid (ext. surface)

$A_{\text{geom}} \times \text{Reflectivity}$

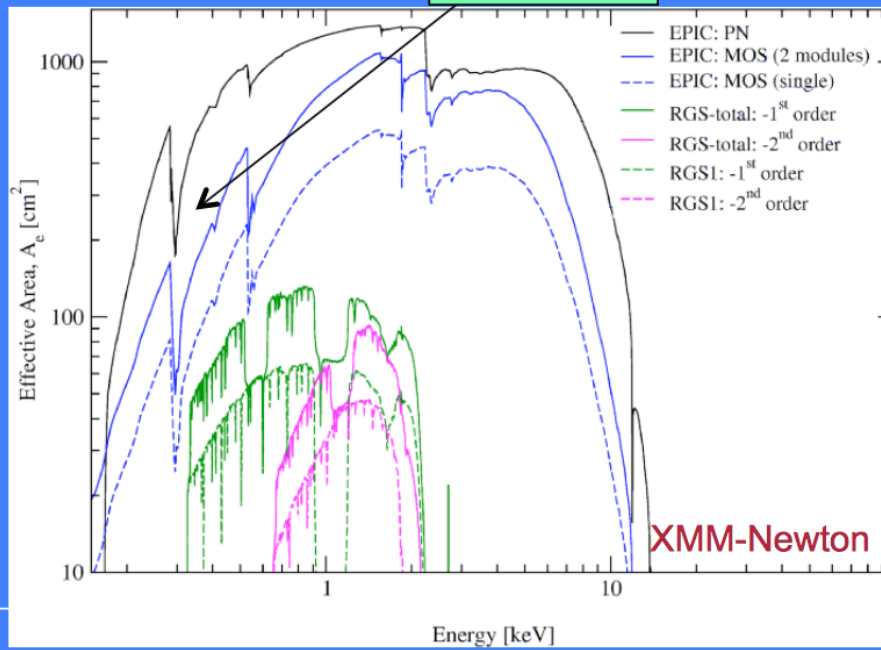


QE



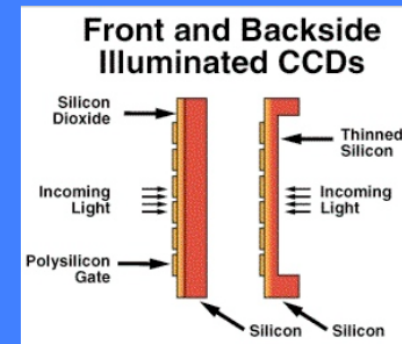
\times

$A_{\text{effective}}$

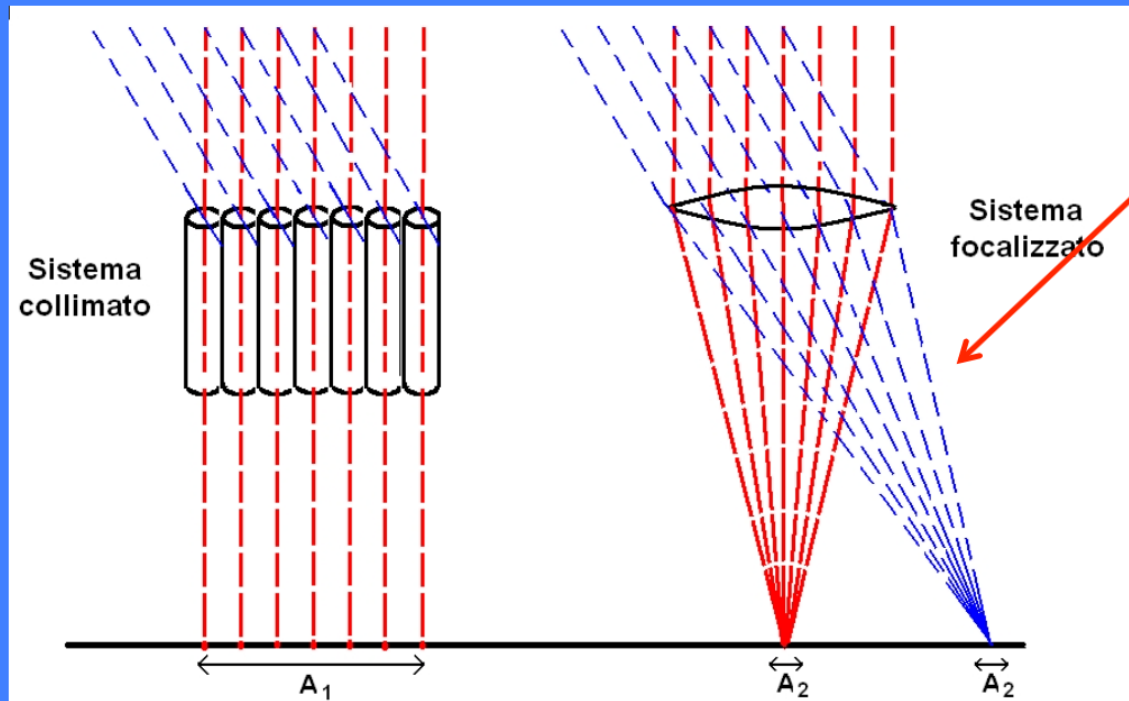


$=$

CCD



Focalizzazione vs collimazione



Proper
imaging
of X-rays
below 20-40 keV

A_d = PSF projected
on the focal plane

$$F_{\min} \approx n_{\sigma} \frac{\sqrt{2B}}{\sqrt{A_{\text{det}} T_{\text{int}} \Delta E}}$$

$$F_{\min} \approx n_{\sigma} \frac{\sqrt{BA_d}}{A_{\text{eff}} \sqrt{T_{\text{int}} \Delta E}}$$

Sistema collimato: limita la regione di cielo da cui puo' provenire un segnale, (quindi limita il background), non incrementandone la "densita"

Sistema focalizzato: fa corrispondere ad ogni sorgente un punto nel piano focale, e "concentra" il segnale, producendo un'immagine

$$C_S = S_E A_e \Delta E \Delta t \eta_E$$

Detected signal

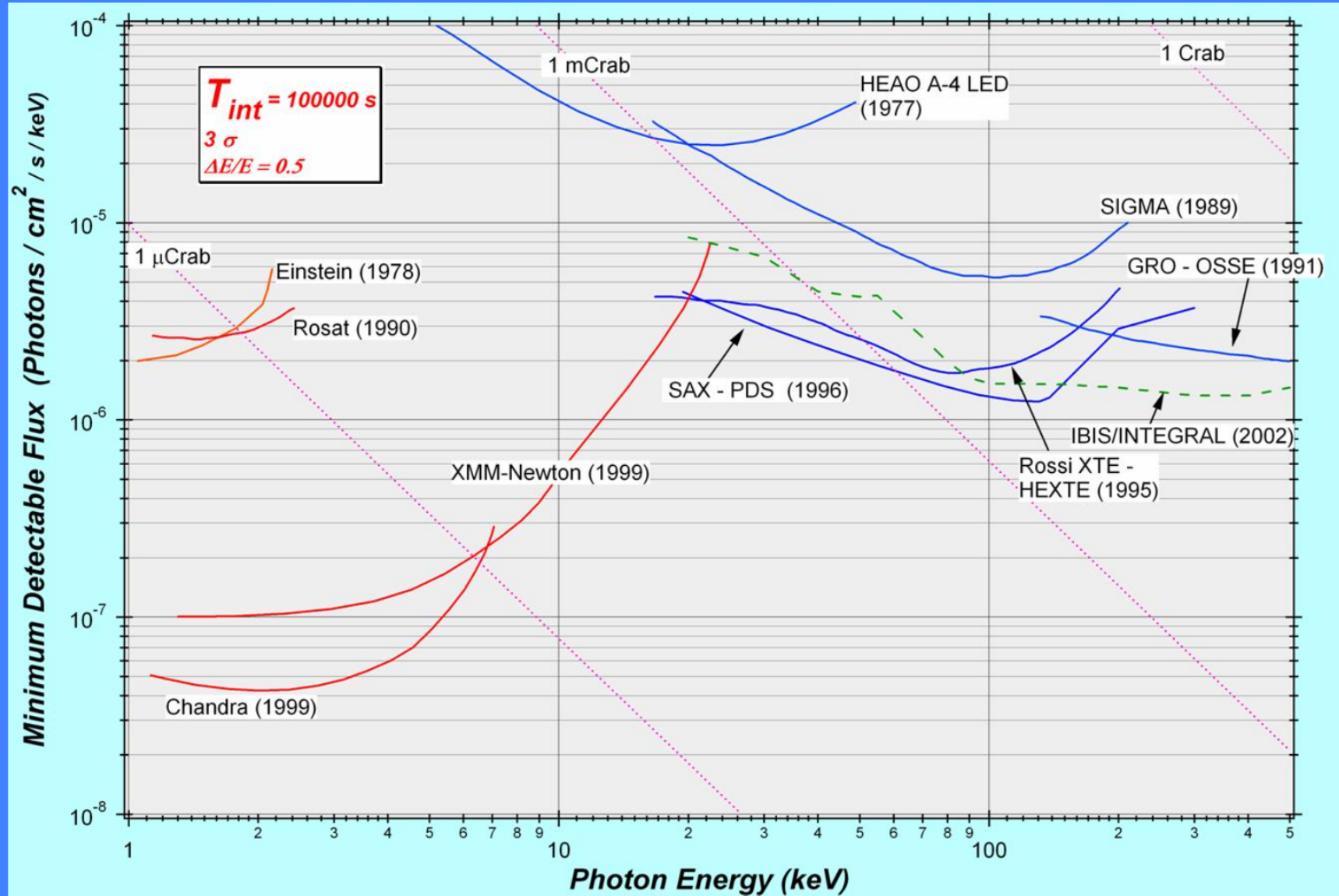
$$C_B = B \varepsilon A_d \Delta E \Delta t$$

Background signal (ε : region of the detector where B counts are focused)

$$S/N = n_\sigma = \frac{C_S}{\sqrt{C_S + 2C_B}} \approx \frac{S_E A_e \Delta E \Delta t \eta_E}{\sqrt{2B \varepsilon A_d \Delta E \Delta t}}$$
$$S_{E,\min} = \frac{n_\sigma}{\eta_E} \frac{1}{A_e} \sqrt{\frac{2B \varepsilon A_d}{\Delta t \Delta E}}$$

Weak sources

Old slide but *Chandra* and *XMM-Newton* still working



X-ray spectroscopy

Telescopes and instruments

Dispersing elements – Bragg Crystal spectroscopy/1

(more details on dispersive spectrometers: Giacconi & Gursky, p. 81-90)

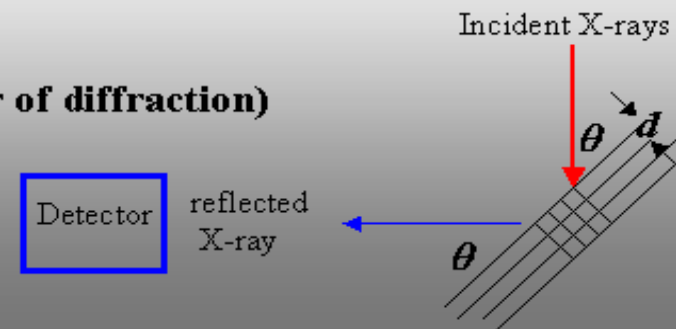
The reflection of X-rays from a crystal lattice follows the Bragg's law, and therefore the name Bragg spectrometer is usually given to the device with this kind of reflection grating.

Here the macroscopic shaping (grooves) of a metallic plate, which is used in longer wavelengths, is replaced by a material with regular lattice structure of atoms (crystal material). The reflection takes place by the same principle as from a macroscopic lattice, leading to a wavelength-dispersed output from a white light input.

The lattice of the crystal forms a 3-dimensional diffraction array which reflects X-rays of wavelength λ within a narrow range of wavelength satisfying the Bragg condition

$$n \lambda = 2d \sin\theta \quad , \quad n = 1, 2, 3, \dots \text{ (order of diffraction)}$$

where d is the crystal lattice spacing.
In practice, order $n=1$ is used.



X-ray spectroscopy

Dispersing elements – Diffraction gratings/1

Ordinary diffraction gratings can also be used from from long wavelengths up to soft X-rays (< 1 keV, in practice).

The grating equation is

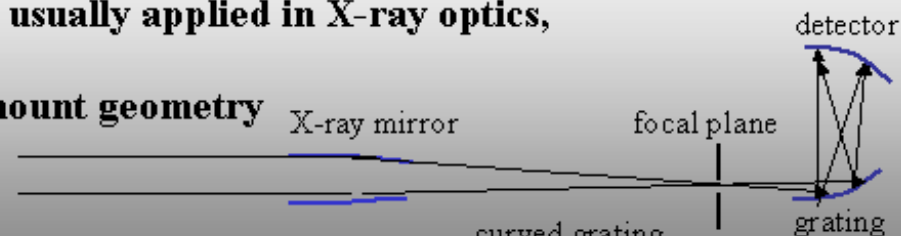
$$n \lambda = (1/N) (\sin \theta - \sin \theta_0), \quad n = 1, 2, 3, \dots \text{ (order of diffraction)}$$

where N is the grating constant (lines/cm), θ is the diffraction angle and θ_0 is the angle of incidence. For X-rays this is usually rearranged in form valid for small angles

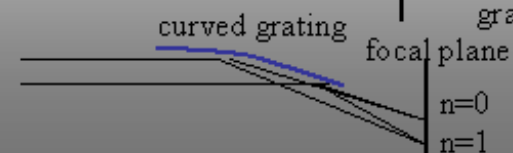
$$n \lambda N = \theta - \theta_0$$

There are two geometries usually applied in X-ray optics,

1. Conventional Johann mount geometry



2. Curved grating producing a line image



Single photon calorimeter

Individual X-ray photons are absorbed by a crystal which is maintained at a T very close to absolute zero (<0.1 K).

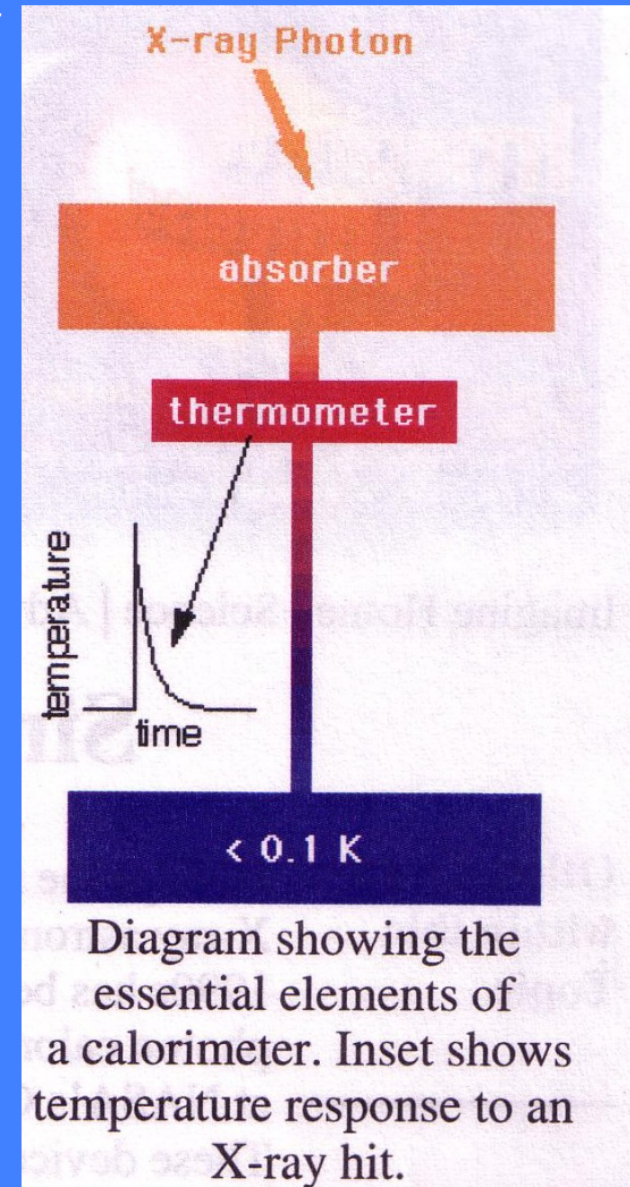
→ 2-3 year lifetime

We measure the increase of T which is proportional to the energy of the X-ray photon

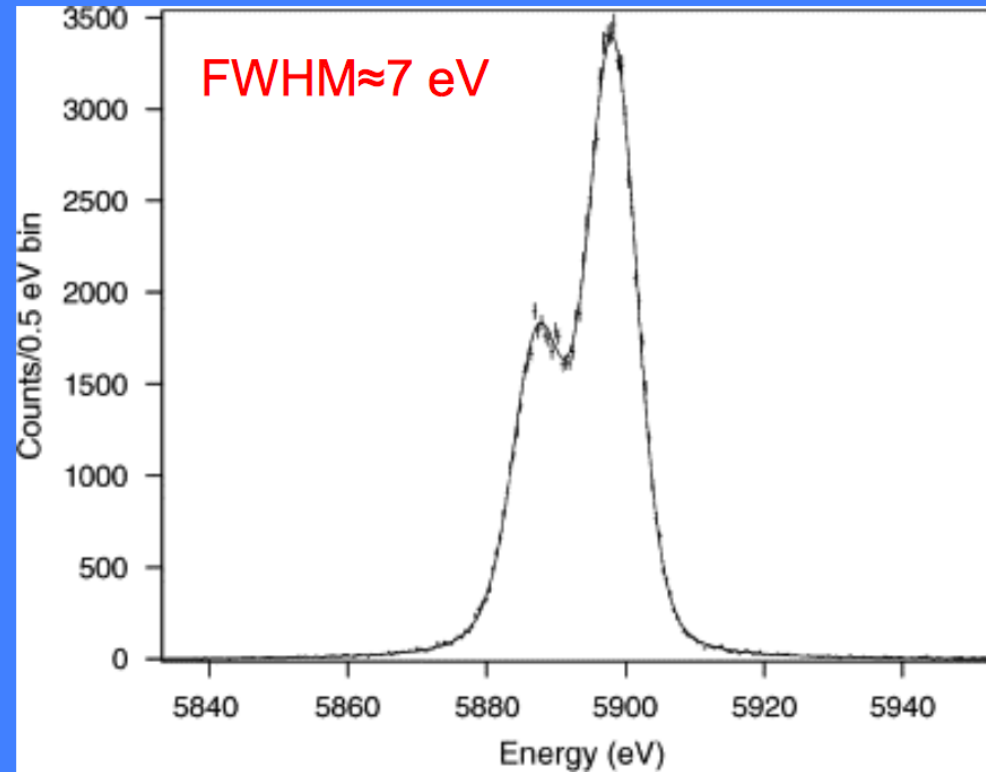
Energy resolution ~ 3 eV

High efficiency

The best spectral resolution of any non-dispersive (grating) spectrometer



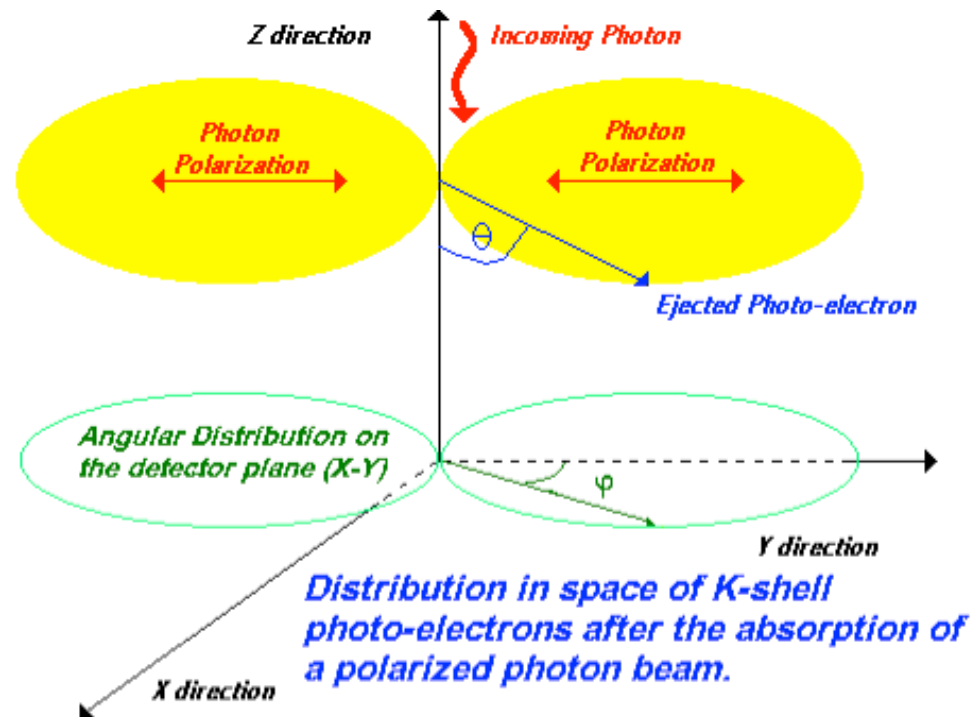
Onboard *Suzaku* – calibration source (^{55}Fe)



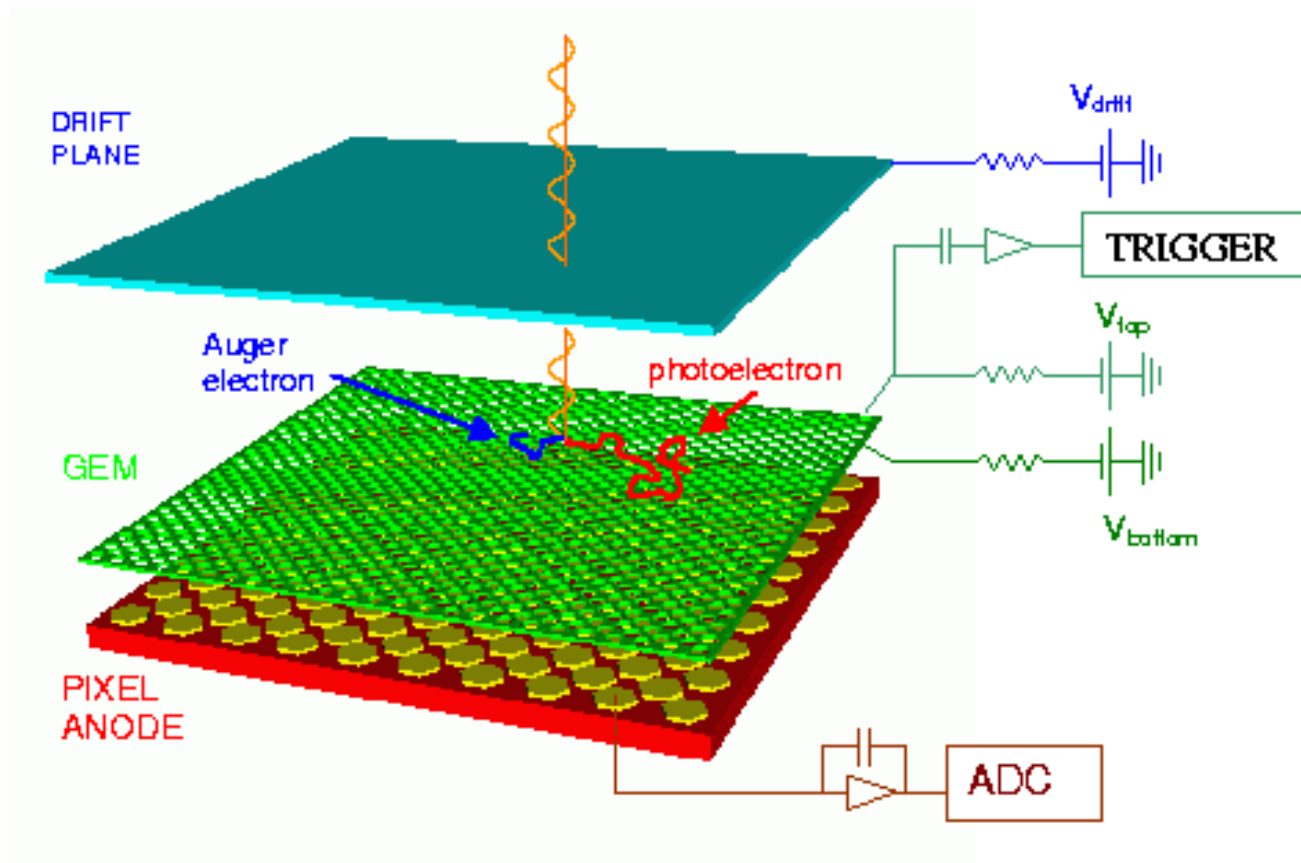
Expected spectral resolutions $\leq 2\text{-}3$ eV in next-generation X-ray calorimeters (e.g., *Athena*)

Onboard of the Japanese mission *ASTRO-H/Hitomi* (Last year ☹)

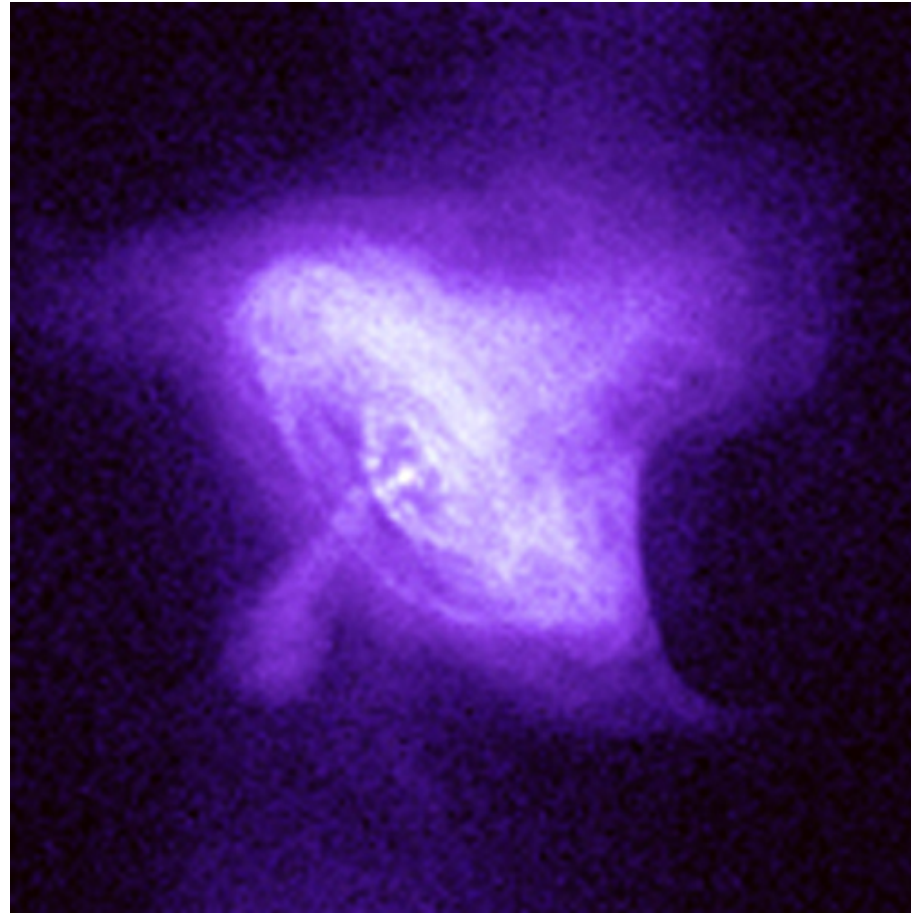
X-ray polarimetry



X-ray polarimetry

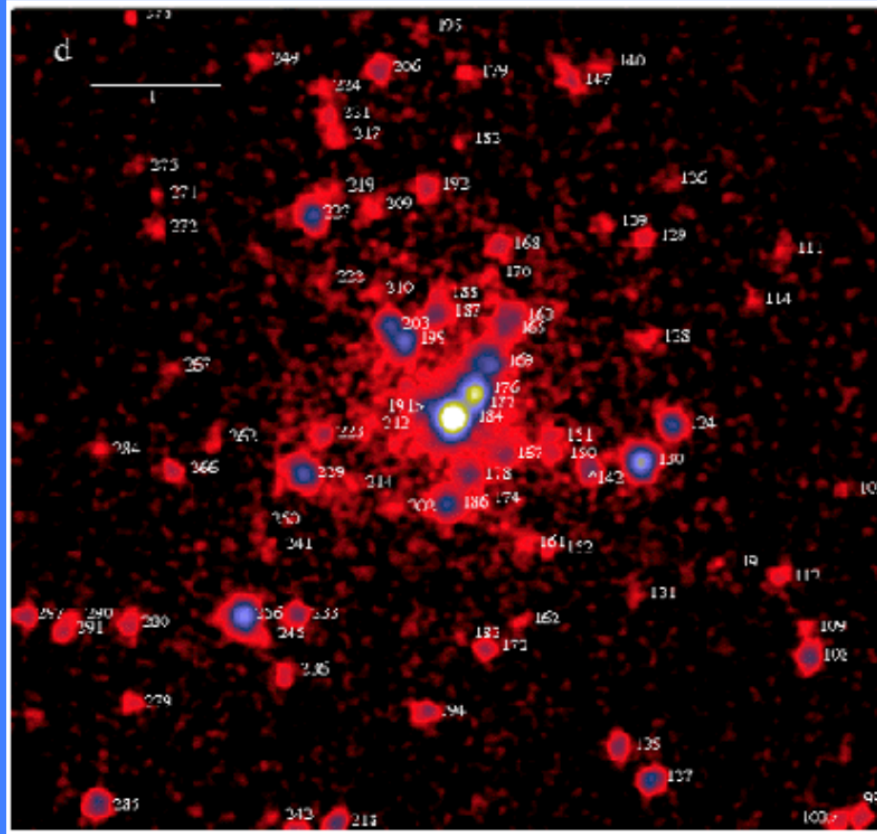


X-ray imaging

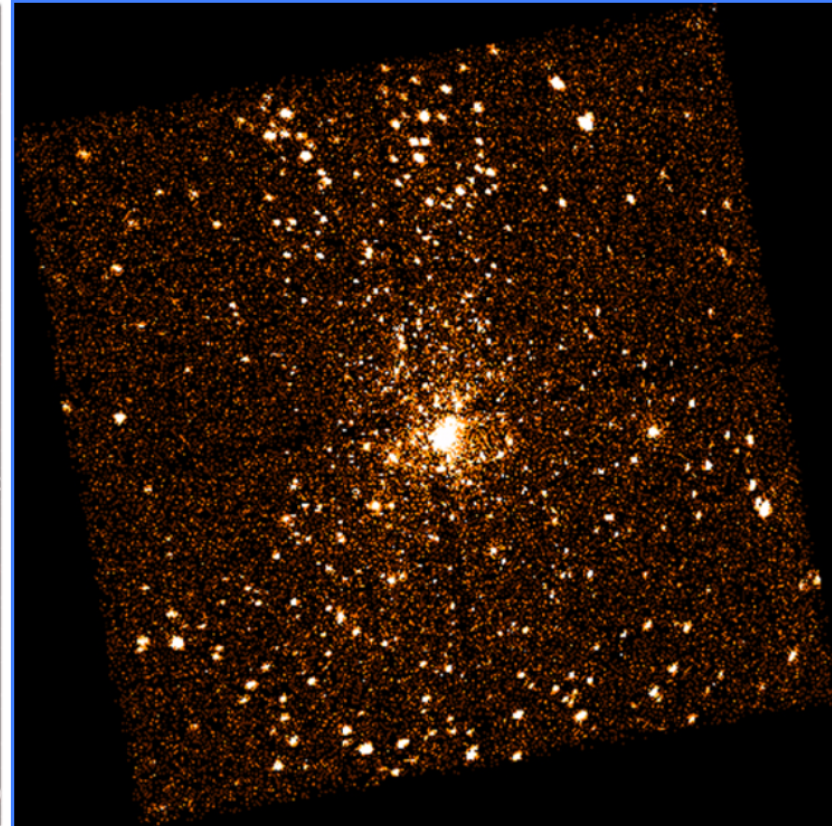


Crab nebula, 2.5", 0.3 – 3 keV

La risoluzione angolare in astronomia X: da *ROSAT* a *Chandra*

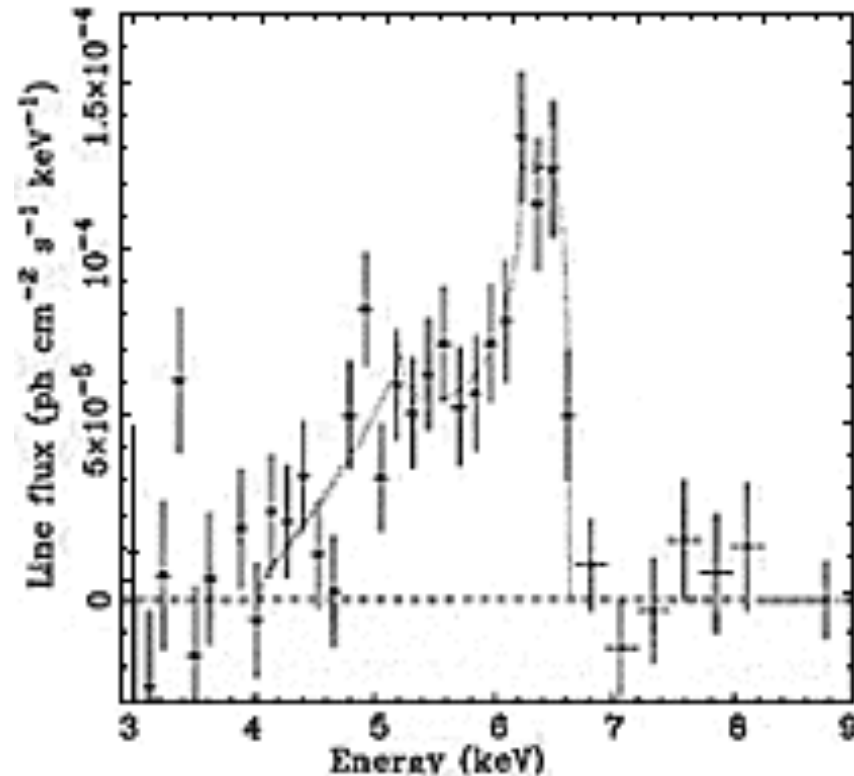


Osservazione di Orion
con ROSAT HRI (47 ks)



Osservazione di Orion
con Chandra ACIS (13.7 ks)

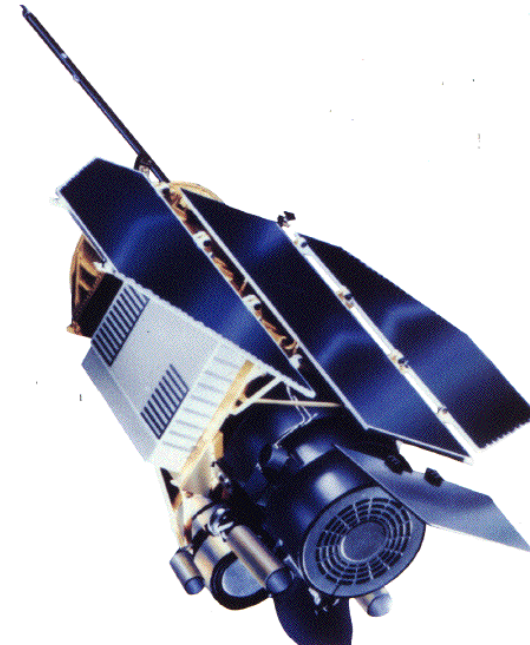
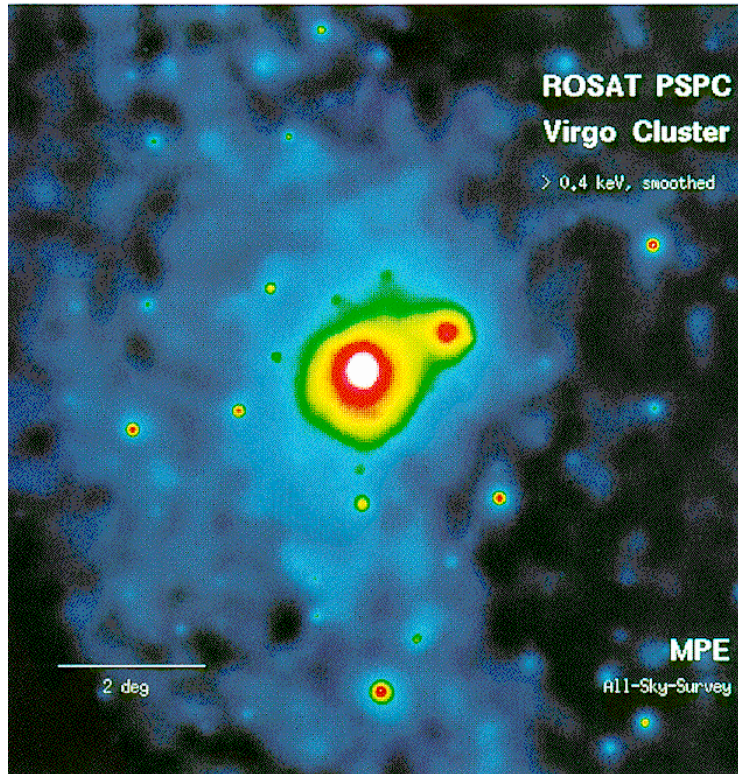
X-ray spectroscopy



The Fe line profile of K-alpha in the X-ray emission from the active nucleus of the galaxy MCG 6-30-15 in the constellation Centaurus is powered by matter accreting into a black hole. 69

ROSAT

<http://www.mpe.mpg.de/xray/wave/rosat/>



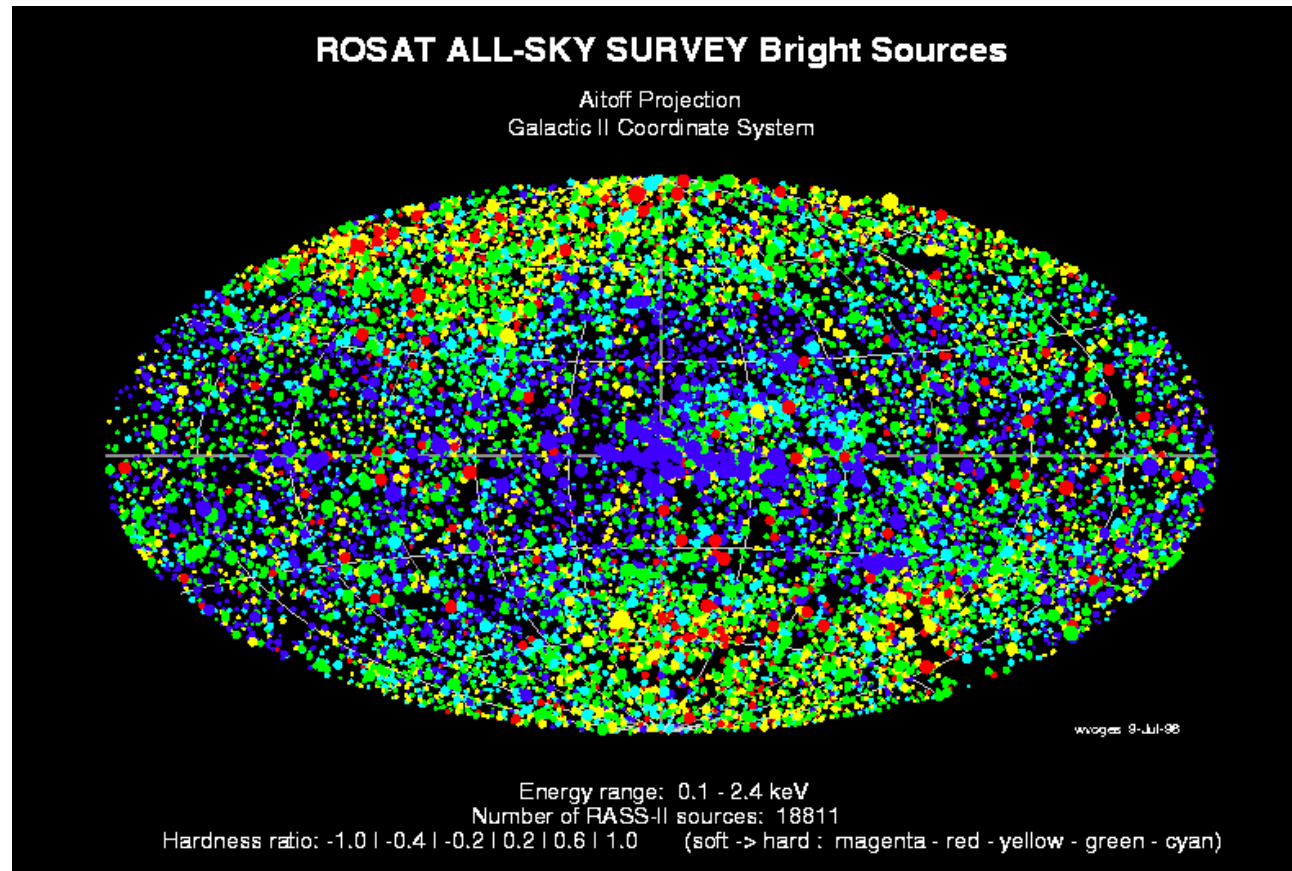
The scientific payload consists two coalligned scientific experiments, the [The X-Ray Telescope](#) which is used in conjunction with one of the focal plane instruments:

- [The Position Sensitive Proportional Counter](#)
- [The High Resolution Imager](#)

and the [The Wide Field Camera](#) which has its own mirror system and star sensor.

ROSAT provides a ~ 2 degree diameter field of view with the PSPC in the focal plane, and ~ 40 arcmin diameter field of view with the HRI in the focal plane. The ROSAT mission began with a six-month, all-sky PSPC survey, after which the satellite began a series of pointed observations that continued for the duration of the project.

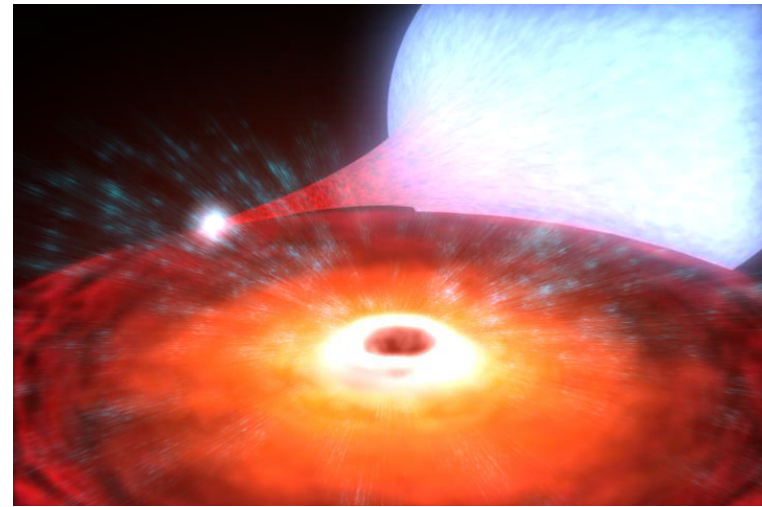
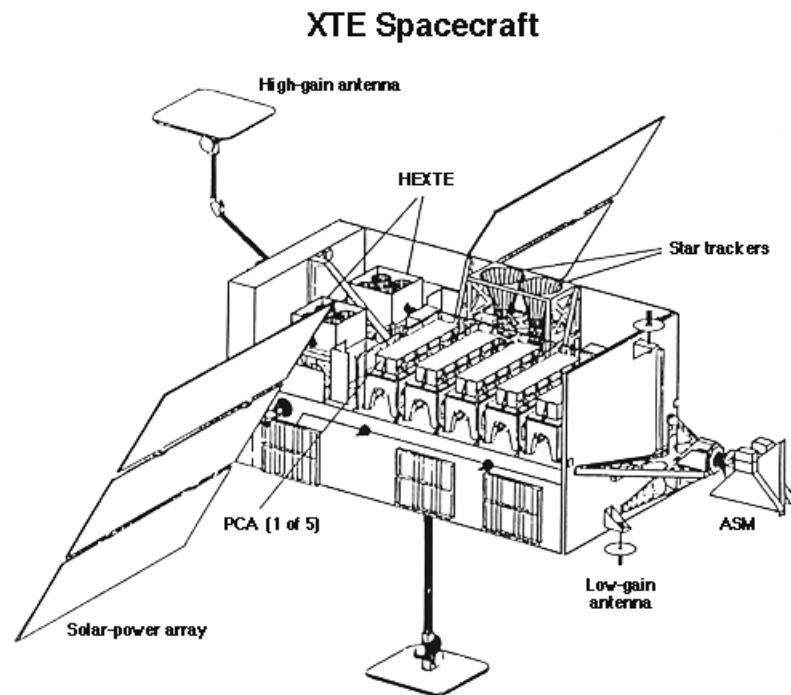
ROSAT results



The ROSAT All-Sky Survey Bright Source Catalogue (RASS-BSC, revision 1RXS) is derived from the all-sky survey performed during the first half year of the ROSAT mission in 1990/91. 18,811 sources are catalogued, with a limiting ROSAT PSPC countrate of 0.05 cts/s in the 0.1-2.4 keV energy band. 71

RXTE

<http://heasarc.gsfc.nasa.gov/docs/xte/xtegif.html>

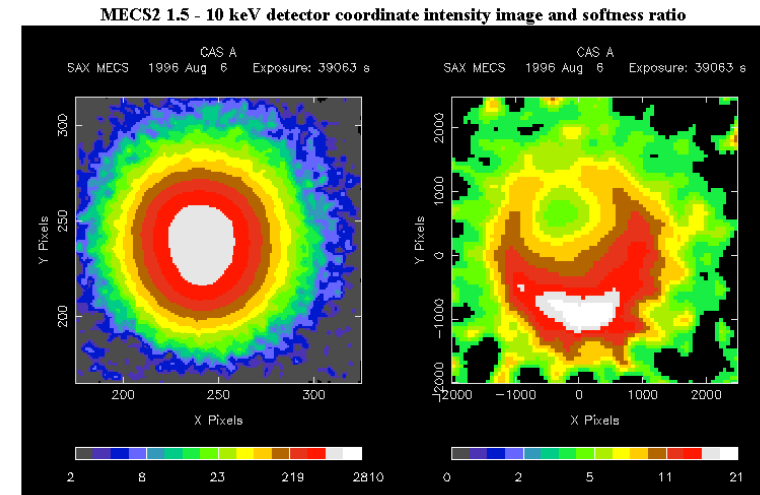
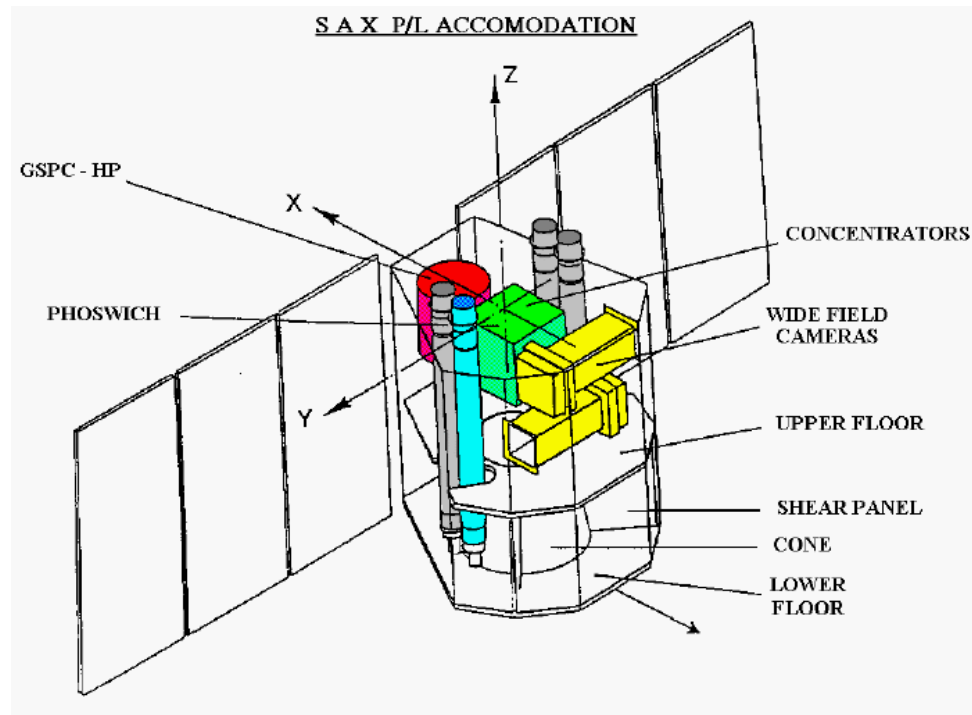


The lowest-mass known black hole belongs to a binary system named XTE J1650-500. The black hole has about 3.8 times the mass of our sun, and is orbited by a companion star

The Rossi X-ray Timing Explorer (RXTE) was launched on December 30, 1995. RXTE features unprecedented time resolution in combination with moderate spectral resolution to explore the variability of X-ray sources. Time scales from microseconds to months are covered in an instantaneous spectral range from 2 to 250 keV. Originally designed for a required lifetime of two years with a goal of five, it operated up to 2012

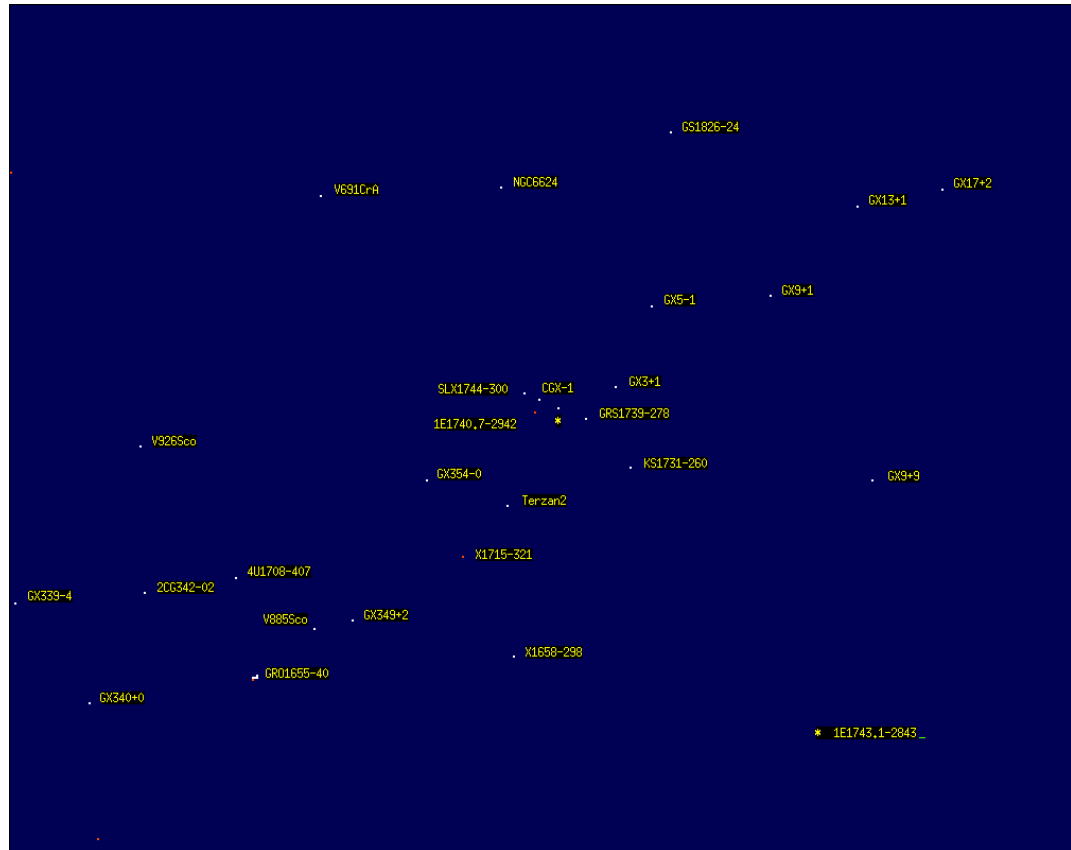
BeppoSAX

<http://www.asdc.asi.it/bepposax>



- Energy Range 0.1 to 200 keV
- Imaging capabilities (1') in the range of 0.1-10 keV.
- High energy (3-300 keV)
- Narrow fields and point in the same direction (Narrow Field Instruments, NFI).
- Monitoring large regions of the sky with a resolution of 5' in the range 2-30 keV
 - two coded mask proportional counters pointing in diametrically opposed directions perpendicular to the NFI
- Anticoincidence scintillator shields of the PDS will be used as a gamma-ray burst monitor in the range 60-600 keV.

BeppoSAX results

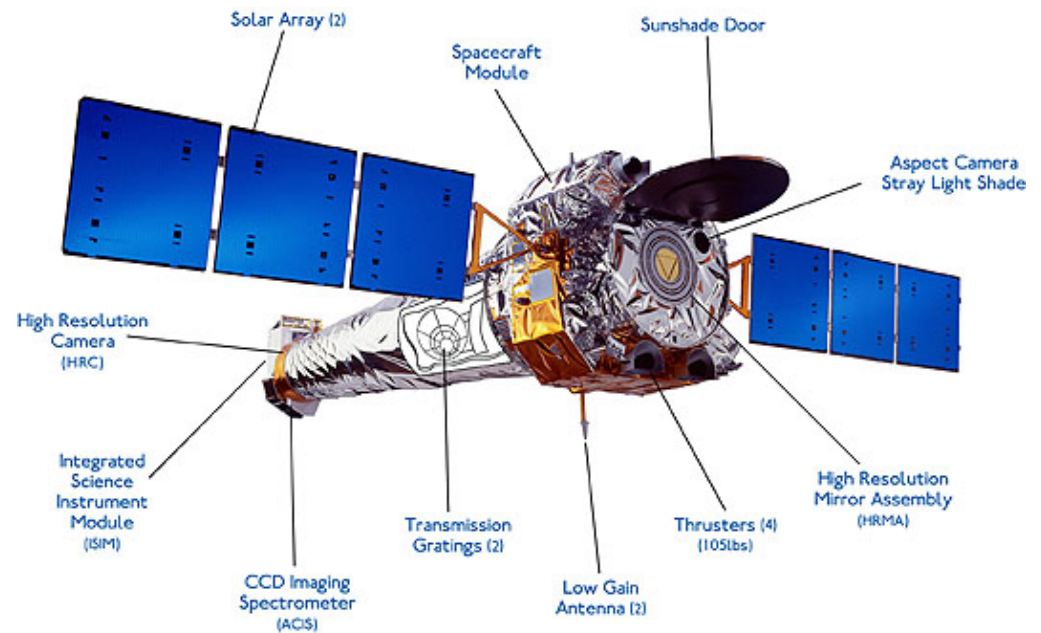


The Galactic Centre has been observed with the Beppo SAX Wide Field Camera 1 (WFC1) in August 1996. Here an image is shown of the 40 degrees by 40. The observation period was from 22-8-1996 07.54 UT through to 23-8-1996 11.38 UT, while the effective exposure totalled about 51 kiloseconds. The number of accepted events was 1.7955×10^7 in the energy range of 5.4 - 11.3 keV. The legenda for the galactic centre source indicated with a yellow star (1E1743.1-2843), is given at lower right in the image.

To our knowledge this is the largest field ever imaged in X-rays in a single pointing.

Chandra X-ray Telescope

<http://chandra.harvard.edu/>



High resolution mirror
two imaging detectors
two sets of transmission gratings.
Spatial resolution: 0.5"
Good sensitivity from 0.1 to 10 keV
High spectral resolution $E/\Delta E = 1000$ 75

XMM-Newton

<http://sci.esa.int/xmm-newton/>



XMM carries the X-ray telescopes with the largest effective area.

58 thin nested mirror shells in each X-ray telescope.

Moderate and high spectral resolution.

Simultaneous optical/UV observations

Spatial resolution: 6"

Energy Range 0.2 to 12 keV

High Spectral resolution at LowE $E/\Delta E = 300$

Wide FoV

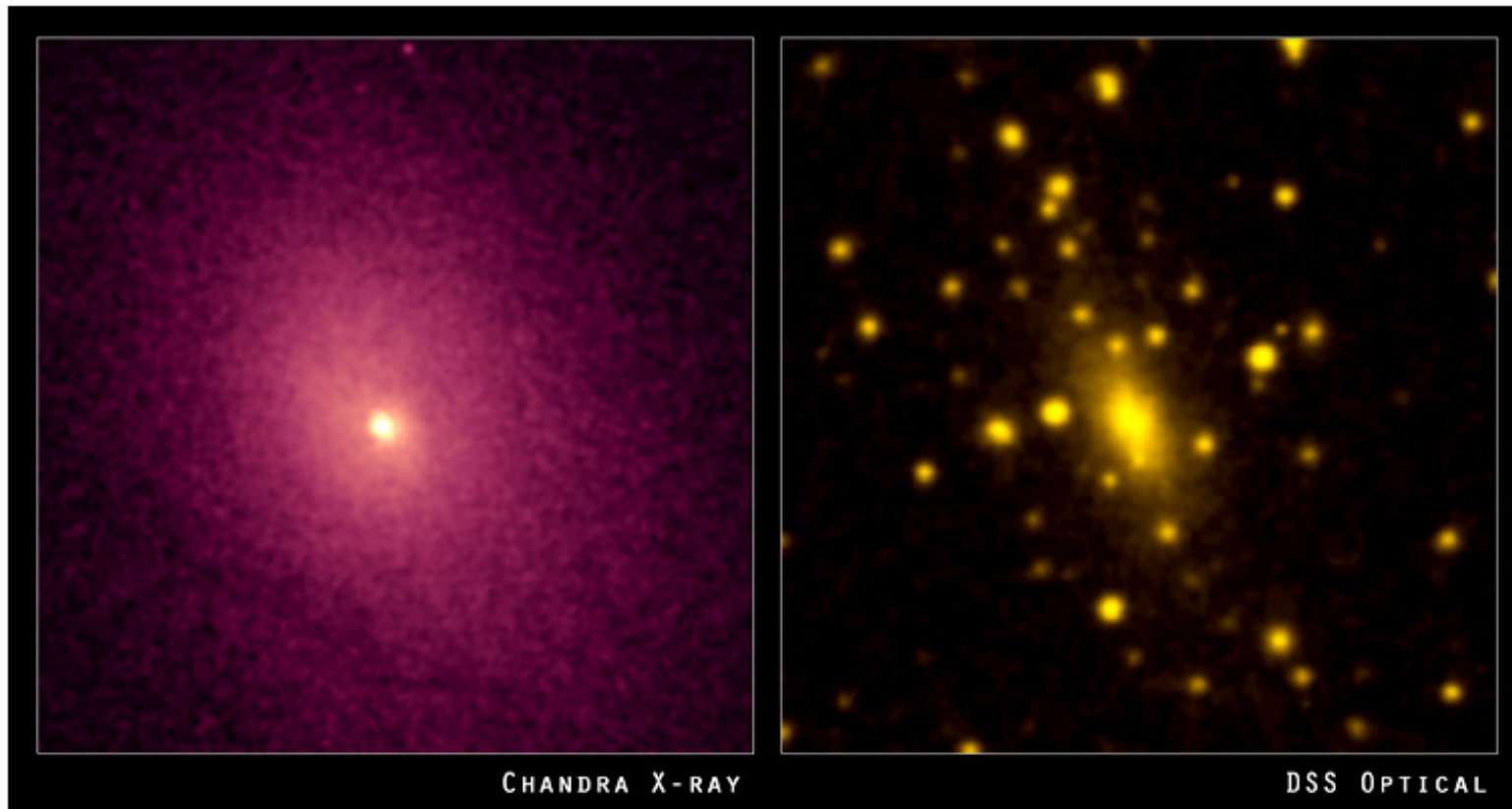
Comparison

A Comparison with other X-Ray Satellites

The following table compares XMM with selected previous X-ray satellites:

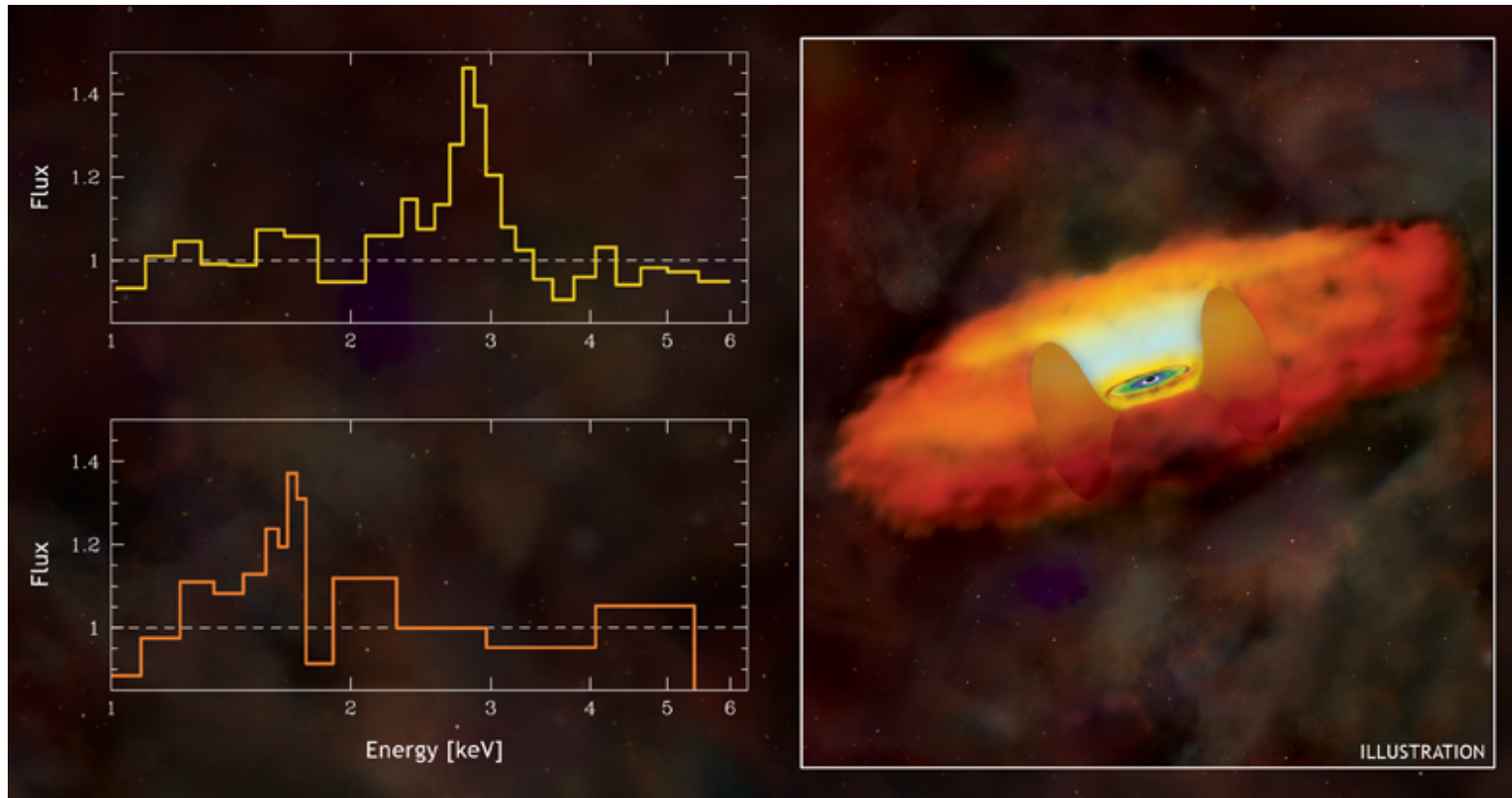
	ROSAT	ASCA	Chandra	XMM
Mirror effective area @ 1.0 keV (cm ²)	400	350	800	4650
Imaging effective area @ 1.0 keV (cm ²)	200	...	400	2400
Spectroscopy effective area @ 1.0 keV (cm ²)	-	-	50	185 (orders 1+2)
Spectroscopic resolving power at 0.5 keV (E/dE)	(1)	9	400-1000	500
Mirror Resolution (arcsec)	3.5	73	0.2	6
CCD energy range (keV)	0.1-2.4	0.5-10	0.1-10	0.1-15
Orbit target visibility (hrs)	1.3	0.9	50	40

Chandra results



The galaxy cluster Abell 2029 is composed of thousands of galaxies (optical image) enveloped in a gigantic cloud of hot gas (X-ray image)

Chandra results



The left side of the above graphic shows portions of X-ray spectra from a subset of 50 black holes about 9 billion light years away (upper panel), and another group of 22 black holes that are about 11 billion light years away (lower panel).

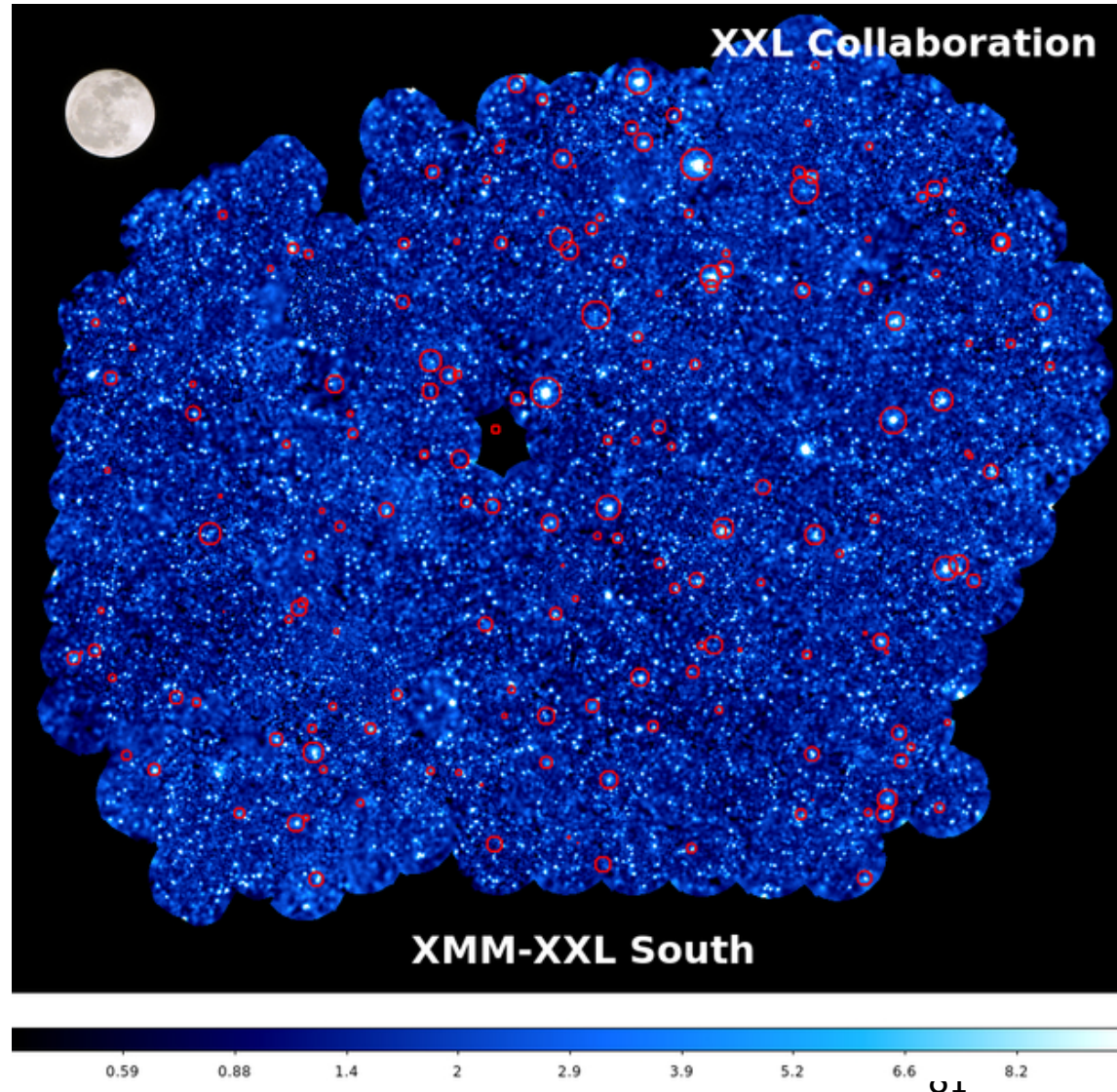
Chandra results



The Tycho and G292.0+1.8 supernova remnants show expanding debris from an exploded star and the associated shock waves. The images of the Crab Nebula and 3C58 show how neutron stars produced by a supernova can create clouds of high-energy particles.

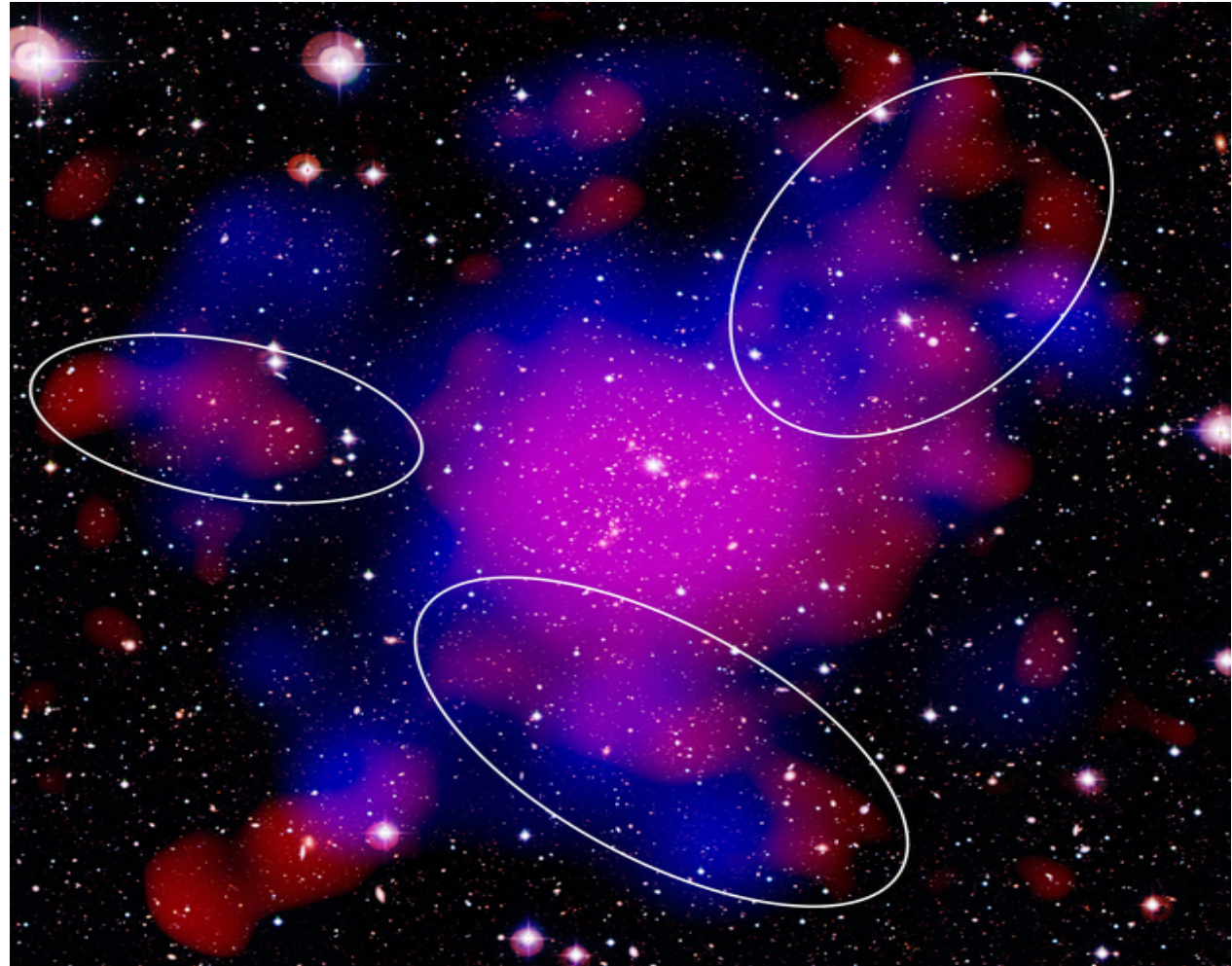
XMM results

- The XXL project, the largest XMM-Newton observing programme to date, set itself the ambitious task of mapping galaxy clusters back to a time when the Universe was just half of its present age. Its aim was to trace the evolution of the large-scale structure of the Universe.



XMM results

Components of the galaxy cluster Abell 2744, also known as the Pandora Cluster: galaxies (white), hot gas (red) and dark matter (blue).



X-ray science highlights

Chandra Images by Category



[Solar System](#) (9 listings)
Comets and planets



[Normal Stars & Star Clusters](#) (30 listings)
Stellar coronas, clusters of stars and hot gas produced by outflow from young stars.



[White Dwarfs & Planetary Nebulas](#) (10 listings)
Hot gas associated with the final stages of evolution of Sun-like stars, novae, and other white dwarfs in binary star systems.



[Supernovas & Supernova Remnants](#) (34 listings)
X-ray sources produced by the violent explosions of massive stars.



[Neutron Stars/X-ray Binaries](#) (26 listings)
Hot, isolated neutron stars, rotation-powered pulsars, and neutron stars accreting matter from a nearby companion star.



[Black Holes](#) (27 listings)
Stellar black holes, mid-mass black holes, and supermassive black holes.



[Milky Way Galaxy](#) (14 listings)
Images related to the Galactic Center and other features of the structure and evolution of the Milky Way Galaxy.



[Normal Galaxies & Starburst Galaxies](#) (39 listings)
Images of spiral, elliptical, and irregular galaxies that show X-ray sources associated with collapsed stars and star formation.



[Quasars & Active Galaxies](#) (33 listings)
Galaxies with unusually energetic activity, including high-energy jets, that is related to a central supermassive black hole.



[Groups & Clusters of Galaxies](#) (33 listings)
Vast clouds of hot gas embedded with numerous galaxies.

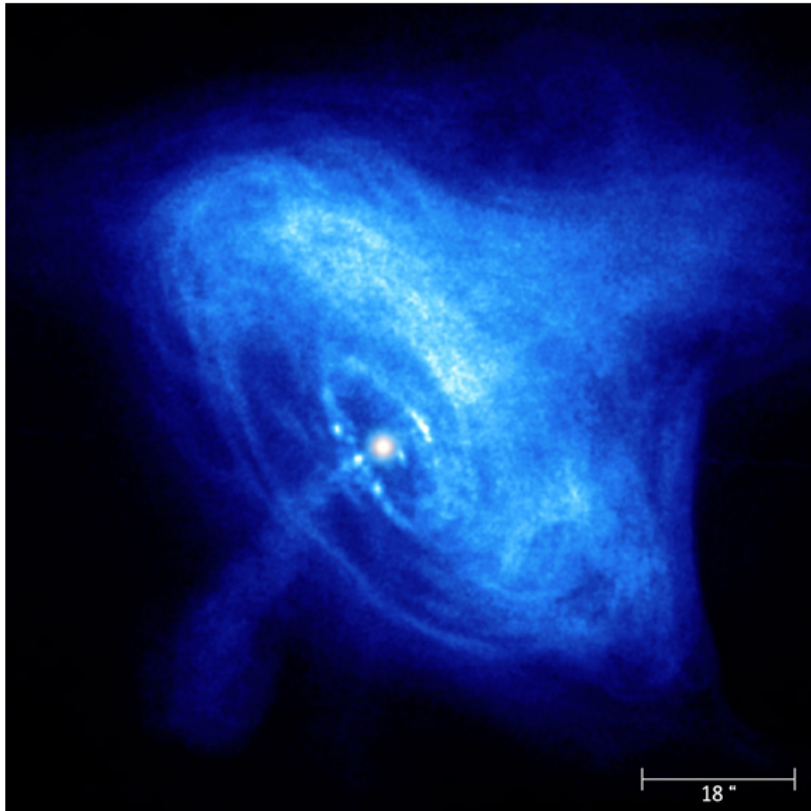


[Cosmology/Deep Fields/X-ray Background](#) (13 listings)
The sky as observed in X-rays is not dark, but gives off a glow thought to be from many distant sources. Deep surveys with the Chandra X-ray Observatory should reveal the cause of this glow.



[Miscellaneous](#) (8 listings)
Objects that don't fit in the above categories, such as brown dwarfs & gamma-ray bursts.

X-ray science highlights



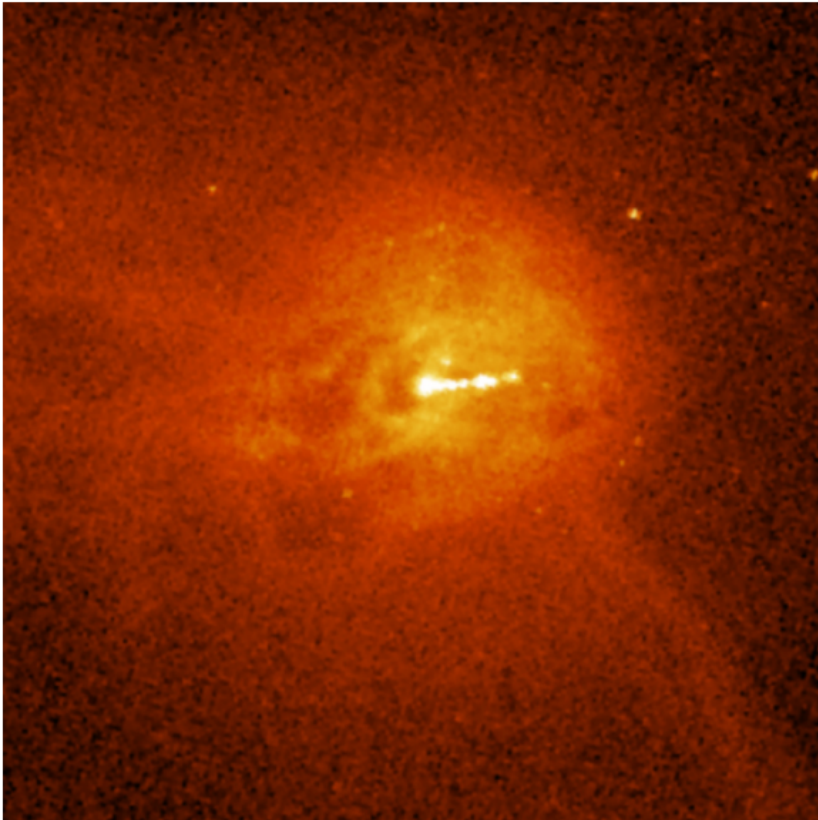
This image provides a view of the activity in the inner region around the Crab Nebula pulsar, a rapidly rotating neutron star seen as a bright white dot near the center of the images.

A wisp can be seen moving outward at half the speed of light from the upper right of the inner ring around the pulsar. The wisp appears to merge with a larger outer ring that is visible in both X-ray and optical images.

- The inner X-ray ring consists of about two dozen knots that form, brighten and fade. As a high-speed wind of matter and antimatter particles from the pulsar plows into the surrounding nebula, it creates a shock wave and forms the inner ring. Energetic shocked particles move outward to brighten the outer ring and produce an extended X-ray glow.

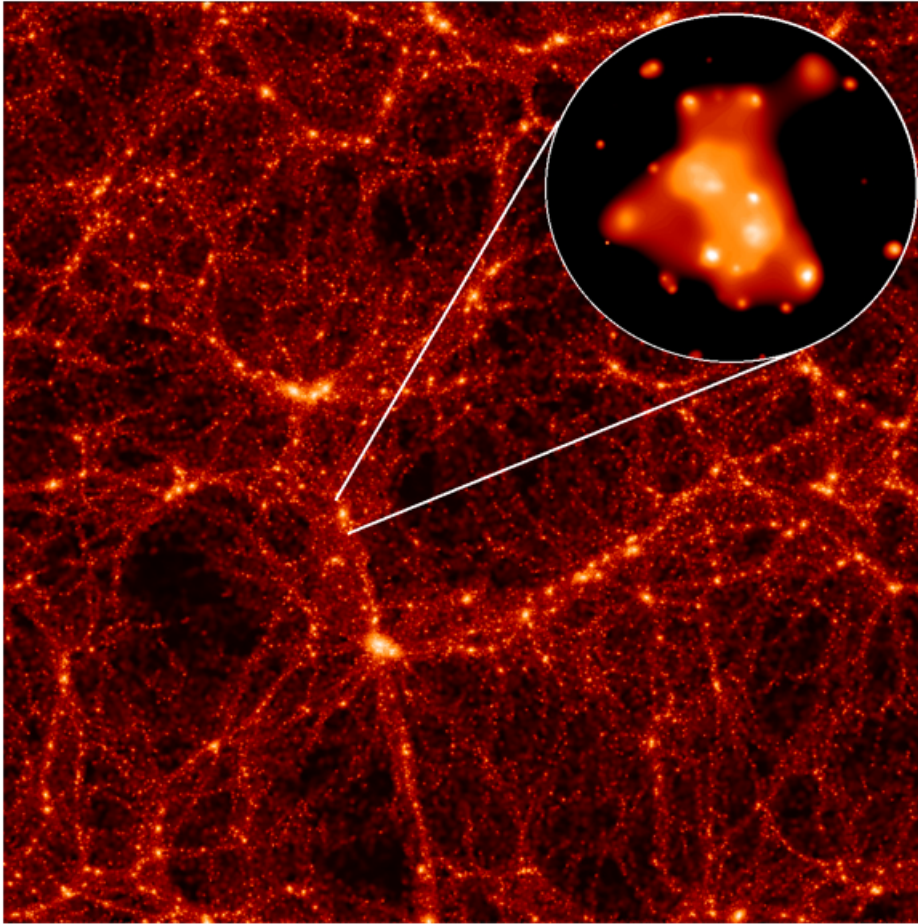
-

X-ray science highlights



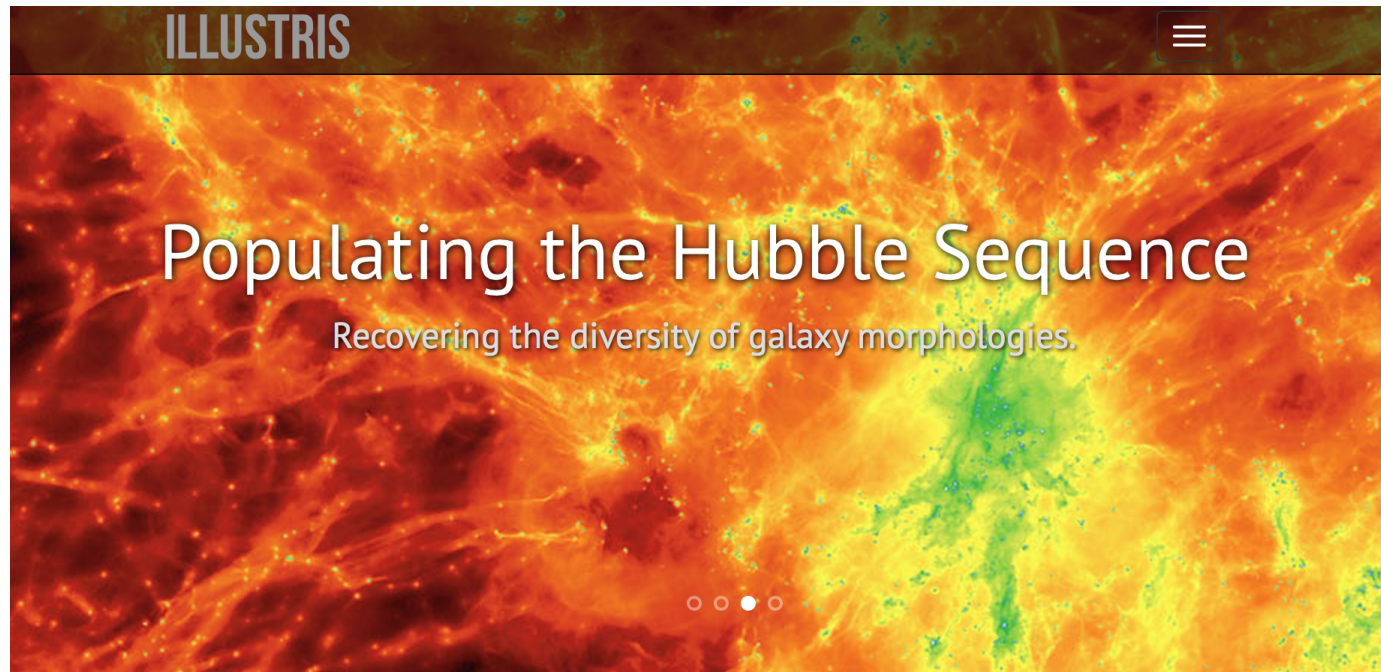
This close-up of M87 shows the region surrounding the jet of high-energy particles in more detail. The jet is thought to be pointed at a small angle to the line of sight, out of the plane of the image. This jet may be only the latest in a series of jets that have been produced as magnetized gas spirals in a disk toward the supermassive black hole

X-ray science highlights



This image shows a computer simulation of a large volume of the Universe. An XMM-Newton X-ray image of a real galaxy cluster from the study is superimposed to illustrate the formation of galaxy clusters in the densest parts of the universe.

Dark Matter and Cosmo Simulations



Welcome

The Illustris project is a large cosmological simulation of galaxy formation, completed in late 2013, using a state of the art numerical code and a comprehensive physical model. Building on several years of effort by members of the collaboration, the Illustris simulation represents an unprecedented combination of high resolution, total volume, and physical fidelity. The [About](#) page contains detailed descriptions of the project, for both the general public and researchers in the field.

On this website we present the scientific motivation behind the project, a list of the collaboration members, key results and references, movies and images created from the simulation data, information on upcoming public data access, and tools for interactive data exploration. The short video below is a compilation made from some of the movies available on the [Media](#) page.

<http://www.illustris-project.org>

<http://www.tng-project.org>

Dark Matter and Cosmo Simulations

Numerical Simulations of the Dark Universe: State of the Art and the Next Decade

Michael Kuhlen^a, Mark Vogelsberger^b, Raul Angulo^{c,d}

^a*Theoretical Astrophysics Center, University of California Berkeley, Hearst Field Annex, Berkeley, CA 94720, USA*

^b*Hubble Fellow, Harvard-Smithsonian Center for Astrophysics, 60 Garden Street, Cambridge, MA 02138, USA*

^c*Max-Planck-Institute for Astrophysics, Karl-Schwarzschild-Str. 1, 85740 Garching, Germany*

^d*Kavli Institute for Particle Astrophysics and Cosmology, Stanford University, Menlo Park, CA 94025, USA*

Abstract

We present a review of the current state of the art of cosmological dark matter simulations, with particular emphasis on the implications for dark matter detection efforts and studies of dark energy. This review is intended both for particle physicists, who may find the cosmological simulation literature opaque or confusing, and for astro-physicists, who may not be familiar with the role of simulations for observational and experimental probes of dark matter and dark energy. Our work is complementary to the contribution by M. Baldi in this issue, which focuses on the treatment of dark energy and cosmic acceleration in dedicated N-body simulations.

Truly massive dark matter-only simulations are being conducted on national supercomputing centers, employing from several billion to over half a trillion particles to simulate the formation and evolution of cosmologically representative volumes (cosmic scale) or to zoom in on individual halos (cluster and galactic scale). These simulations cost millions of core-hours, require tens to hundreds of terabytes of memory, and use up to petabytes of disk storage. Predictions from such simulations touch on almost every aspect of dark matter and dark energy studies, and we give a comprehensive overview of this connection. We also discuss the limitations of the cold and collisionless DM-only approach, and describe in some detail efforts to include different particle physics as well as baryonic physics in cosmological galaxy formation simulations, including a discussion of recent results highlighting how the distribution of dark matter in halos may be altered. We end with an outlook for the next decade, presenting our view of how the field can be expected to progress.